PLG-0276
Revision 1

OYSTER CREEK
TORNADO MISSILE RISK ANALYSIS

Prepared for
GPU NUCLEAR CORPORATION
Parsippany, New Jersey
August 1983

PICKARD, LOWE AND GARRICK, INC.
CONSULTANTS — ELECTRIC POWER
IRVINE, CALIFORNIA WASHINGTON, D.C.

PLG-0276
Revision 1

OYSTER CREEK
TORNADO MISSILE RISK ANALYSIS

by

Pickard, Lowe and Garrick, Inc.
Douglas C. Iden
Harold F. Perla
B. John Garrick

Applied Research Associates, Inc.
Lawrence A. Twisdale
William L. Dunn

Prepared for
GPU NUCLEAR CORPORATION
Parsippany, New Jersey
August 1983

PICKARD, LOWE AND GARRICK, INC.
CONSULTANTS — ELECTRIC POWER
IRVINE, CALIFORNIA WASHINGTON, D.C.

TABLE OF CONTENTS

LIST OF TABLES AND FIGURES

1. INTRODUCTION

The purpose of this report is to document the results of a tornado missile risk analysis of selected structures at the Oyster Creek Nuclear Generating Station (OCNGS). This report is part of GPU Nuclear's (GPUN) response to Systematic Evaluation Program (SEP) Topic III-4.A, Tornado Missiles, Sections 4.6.1 and 4.6.2 of the Nuclear Regulatory Commission (NRC) integrated assessment. The risk analysis is limited to the following structures and components:

- Emergency diesel generators and fuel oil day tank.
- Mechanical equipment access area and the safety related equipment in the vicinity of the railroad airlock on the 23-foot elevation of the reactor building.

The objectives of this risk analysis are to determine the frequency of tornado missiles causing damage to the above structures and components and to evaluate the consequences in terms of core melt frequency.

The analysis approach is summarized in Section 2. A summary of the results is presented in Section 3. The detailed tornado missile wind hazard and penetration analysis performed by Applied Research Associates, Inc., is included as Section 4. Section 5 contains the detailed tornado missile consequences analysis in terms of its impact on core melt frequency. Section 6 is a list of the references.

2. ANALYSIS APPROACH

To meet the objectives of this analysis the following approach was taken making maximum utilization of previously documented reports:

- Perform Tornado Wind Hazard Analysis. The probability distribution of tornado windspeed versus frequency of exceedance per year was revised from previously developed regional tornado data (Reference 1 and reproduced in the Appendix).

- Perform Tornado Missile Penetration Analysis. The frequency of tornado missile impact and damage was evaluated for the diesel generator and fuel oil day tank compartments, the diesel fuel oil supply tank compartment, and the reactor building railroad airlock doors and walls based on a site specific model of the plant layout including targets and postulated sources of missile types.

- Perform Tornado Missile Consequences Analysis. The frequency of core melt from tornado missile damage to these structures and components was evaluated using a plant specific model. It is not unlikely that a tornado in the vicinity of the plant site would strike the transmission lines to the plant or the associated substations and thereby cause a loss of offsite power. Therefore, the loss of offsite power event sequence diagram and event tree from Reference 2 were used to model the scenarios. Plant specific data from References 2 and 3 were also used.

3. SUMMARY OF RESULTS

Tornado missiles having the potential to disable the emergency diesel generators, fuel oil day tank, fuel oil supply tank, or safety related equipment in the vicinity of the mechanical equipment access area (reactor building railroad airlock) have a negligible contribution to the Oyster Creek core melt frequency using conservative assumptions and estimates. The estimated contribution to the total Oyster Creek core melt frequency is about 1.4×10^{-7} per reactor year which is less than 0.2% of the proposed NRC core melt frequency safety goal. If the railroad airlock inner doors were always closed as opposed to always open, the tornado missile contribution to core melt frequency would be even less noticeable.

Two specific targets were found to be susceptible to tornado missiles although both had low penetration frequencies (less than 1.0×10^{-5} per reactor year).

- The diesel generator exhaust stack openings (about a 7-foot diameter hole in the top of each compartment) have a tornado missile penetration frequency of less than 1.0×10^{-7} per reactor year for each opening. This result is an upper bound conservative estimate because all tornado missile hits in either exhaust stack opening were modeled with no stack perforation resistance and, hence, vertical missile impact is assumed to be equivalent to missile entrance into the diesel generator compartment. In addition, there was no penetration or scabbing damage to any other part of the diesel generator compartment walls, roof, fuel oil supply tank/day tanks, or intake/exhaust roof gratings. This result (no damage) is typical for these reinforced concrete structures and steel gratings. The frequency of tornado missiles just hitting or landing on the intake or exhaust gratings is in the range of 1.0×10^{-9} to 2.8×10^{-8} per reactor year. The low grating hit frequencies (with no penetration) are mainly due to the rooftop location of the gratings and their relatively small size (160 square feet) since missiles originating near grade level must be lifted by the winds and dropped onto the gratings. Further, should a missile land on the grating, it is not likely that the intake structure would be significantly blocked or that the exhaust would be inhibited. Therefore the diesel generator failure frequency from tornado missiles is dominated by the conservative frequency of missiles hitting the exhaust stack opening.

- The reactor building tornado missile entrance frequency via the mechanical equipment access area (railroad airlock) is about 6.0×10^{-6} per reactor year. This result is an upper bound conservative estimate considering the directional tendencies of tornadoes, the orientation of the airlock structure, and the presence of adjacent structures (shadowing). The model for this target assumes that the inner railroad airlock doors are always open. Additional targets were modeled which give us insight regarding the effect of having the inner doors closed all the time. The results of this additional analysis indicate that with the inner doors closed, no missiles will penetrate these doors and enter the reactor building

(the impact or hit frequency for the inner doors is about 2.5×10^{-6} per reactor year which is within a factor of 2.4 of the above conservative results for hitting the outer doors, 6.0×10^{-6} per reactor year. The frequency of 2.5×10^{-6} per reactor year is probably a more realistic penetration frequency.

The impact of the above tornado missiles and associated high winds is assumed to result in a concurrent loss of offsite AC power to Oyster Creek since the electrical substations and transmission lines are very susceptible to the tornado winds and missiles which penetrate these structures and components. Therefore, the following scenarios are evaluated in the context of a loss of offsite AC power initiating event using the event sequence and event tree plant models in Reference 2:

- Scenario 1. Tornado winds and missiles induce a loss of offsite AC power which also disables both diesel generators with an initiating event frequency of 1.0×10^{-7} per reactor year. It is assumed that tornado missiles which penetrate a diesel generator exhaust stack opening disable the diesel with a conditional frequency of 1.0. In addition, the conditional frequency of the second diesel generator failing given the first has already failed is also assumed to be 1.0. After propagating through the loss of the offsite AC power plant model, the resultant core melt frequency from this scenario is 1.0×10^{-11} per reactor year, which has a negligibly small and unnoticeable contribution to the total core melt frequency when compared to the results presented in Reference 2 or the proposed NRC core melt frequency safety goal.

- Scenario 2. Tornado winds and missiles induce a loss of offsite AC power which also disables safety related equipment in the vicinity of the mechanical equipment access area (23-foot elevation of the reactor building just inside the railroad airlock) with a frequency of 6.0×10^{-6} per reactor year. It is conservatively assumed that the missiles entering the building will damage the DC-1 motor control center, 1AB21B and 1AB21A motor control centers, the control rod drive system (the scram system is still operable), and the containment spray system with a failure frequency of 1.0. After propagating through the loss of the offsite AC power plant model, the resultant contribution to core melt from this scenario is 1.4×10^{-7} per reactor year, which has a very small contribution (less than 0.2%) to the core melt frequency results presented in Reference 2 or to the proposed NRC core melt frequency safety goal. Since as noted earlier, with only the inner doors closed, no missiles are calculated to even enter the reactor building, therefore, this already small contribution can be easily eliminated or significantly reduced by keeping the inner doors closed all or most of the time.

In addition to the above scenarios, the potential for failure of the diesel generator roof panels due to tornado missile impacts was evaluated. This evaluation is included as Section III.C of the Applied Research Associates, Inc., report (Tab 4). The results from this evaluation show that, even using a conservative upper bound estimate of

effective impact velocity, the exceedance frequency greater than 1.0×10^{-7} is less than 75 feet per second. Failure of the steel channels that support the diesel generator roof panels is estimated to occur at velocities greater than about 80 miles per hour or about 120 feet per second. The exceedance frequency at 120 feet per second is less than 10^{-8} based on this conservative upper bound evaluation. Therefore, this failure mode does not have an impact on the overall contribution of tornado missiles to the total Oyster Creek core melt frequency.

4. TORNADO MISSILE WIND HAZARD AND PENETRATION ANALYSIS

The tornado missile wind hazard and penetration analysis was performed by Applied Research Associates, Inc. Their final report is included in its entirety in this section.

May 1983

Final Report C570

TORNADO MISSILE ANALYSIS OF DIESEL GENERATOR COMPARTMENTS AND REACTOR BUILDING AIRLOCK STRUCTURE AT OYSTER CREEK NUCLEAR GENERATING STATION

Prepared for

Pickard, Lowe and Garrick, Inc.
17840 Skypark Boulevard
Irvine, California 92714

Prepared by

L. A. Twisdale
W. L. Dunn

Applied Research Associates, Inc.
Southeast Division
4917 Professional Court
Raleigh, North Carolina 27609

TABLE OF CONTENTS

I. INTRODUCTION

The objective of this investigation was to estimate tornado windspeed and tornado missile impact and damage probabilities for the diesel generator and airlock structures at the Oyster Creek Nuclear Generating Station. Information on the site location and plant structures was provided by Pickard, Lowe and Garrick, Inc.

The scope of this investigation has consisted of:

1. Tornado Wind Hazard Analysis. Adjustments to the probability distribution of tornado windspeed vs probability of exceedance that was developed in Ref. 1 from regional tornado data [2]. The upperbound windspeeds for F'6 tornadoes was taken as 360 mph, consistent with the NRC Region I tornado criteria [3].

2. Tornado Missile Penetration Analysis. The TORMIS simulation methodology [2,4,5] was used to estimate probabilities of missile impact and damage to the following targets:

   a. Diesel generator compartment and openings
   b. Diesel oil tank compartment
   c. Reactor building railroad airlock doors and walls.

   The Oyster Creek plant structures and missile origin characteristics were modeled similar to the Cable Tray Bridge Analysis [1].

The methodology and tornado data base follow the models and analyses described in Refs. 2 and 4-12. This methodology has been previously summarized in Ref. 1 and is not repeated herein. This report documents the input data and plant target models used in the tornado missile analyses and summarizes the results of the simulation.

II. PROBLEM DESCRIPTION AND SIMULATION INPUTS

A. Plant and Target Specification

The locations of the Airlock Structure (Target 10)and Diesel Generator Compartments (Targets 1-8) are summarized in Fig. II-1, which is a plan view of the main structures at the plant. The plant XYZ inertial reference frame is positioned as before [1]. The Ref. 1 plant model has been slightly modified; for example, the cable tray bridges have been removed (since they are neither a source of missiles nor a significant shield) and the Turbine Bay has been extended to include the Reheater Bay and Mechanical Equipment Room. Also, additional structures have been added to model the targets of interest and nontornado-proof buildings that are likely sources of missiles during a severe tornado strike. The geometric and material parameters of the targets given in Fig. II-1 were obtained from plant drawings and other data provided by Pickard, Lowe and Garrick.

The collection of safety-related targets of interest and other structures forms a set of 22 targets. Data on these targets are summarized in Table II-1 with the following conventions as described in Ref. 2. Target type denotes geometric type according to: 1 = rectangular parallelepiped and 2 = circular cylinder. The reference point is the XYZ point at the base elevation of the southwest corner of each rectangular parallelepiped target and the base elevation of the center of each cylinder. The dimensions WX, WY, and WZ give the modeled building dimensions from the reference point in the x-, y-, and z-directions, respectively, for the rectangular parallelepiped targets; for cylindrical targets, WX is the cylinder radius and WZ is the height of the cylindrical surface. In Table II-1, the surface material designators are: -1 for imaginary, 0 for reinforced concrete, 1 for steel plate.

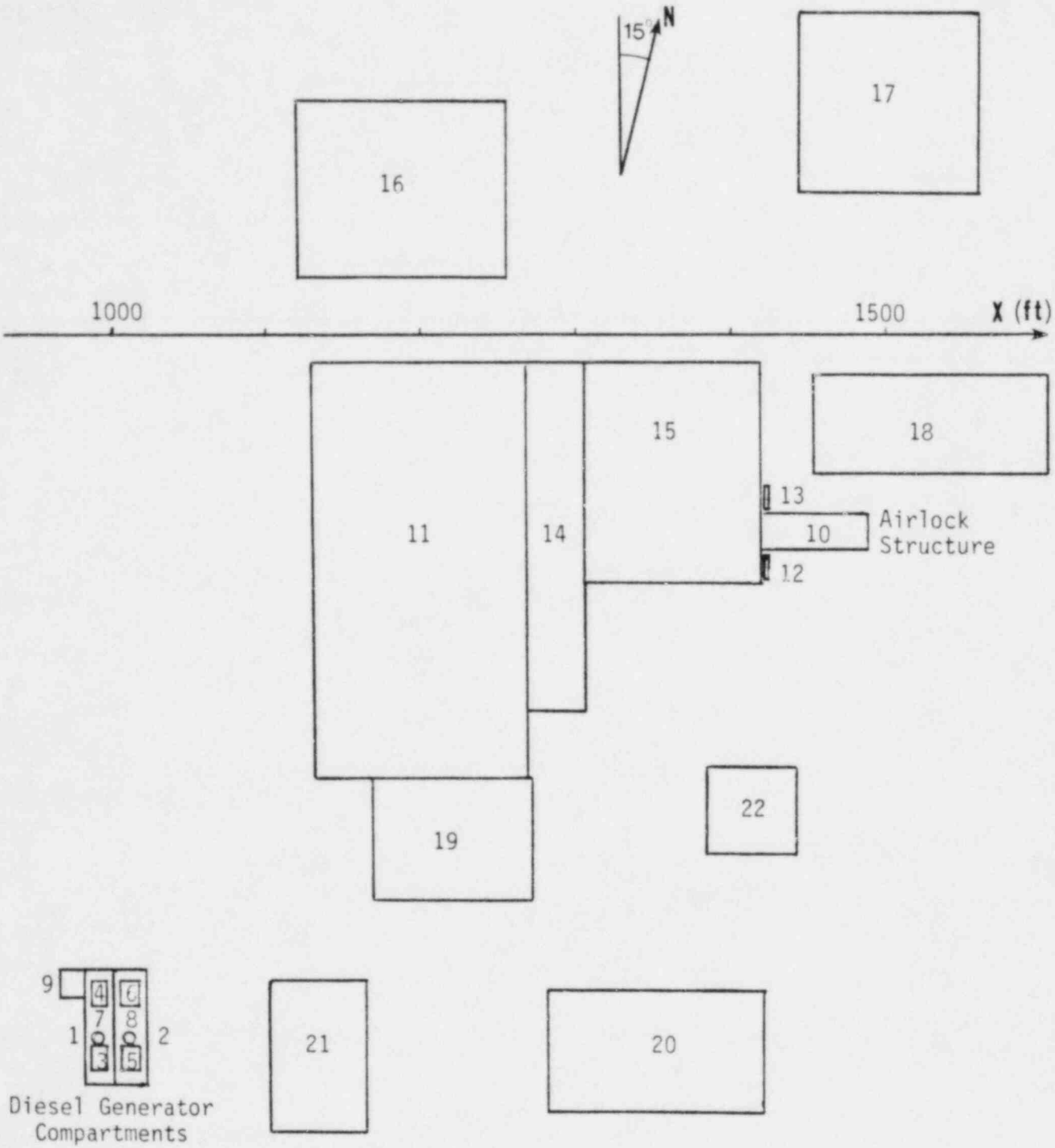

Figure II-1. Plan View of Modeled Plant Targets

TABLE II-1. TARGET LOCATION AND DESCRIPTION

Target									Surface			
			Reference Point (ft)			Dimensions (ft)						
No.	Type[1]	Description	X	Y	Z	WX	WY	WZ	No.[2]	Mat'l[3]	Thk (in)	Strength (psi)
1	1	Diesel Generator-Unit 1	980	-490	0	20	78	14	1	0	18	3,000
									2	0	18	3,000
									3	0	18	3,000
									4	0	18	3,000
									5	0	12	3,000
									6	-1	--	--
2	1	Diesel Generator-Unit 2	1000	-490	0	20	78	14	1	0	18	3,000
									2	0	18	3,000
									3	0	18	3,000
									4	0	18	3,000
									5	0	12	3,000
									6	-1	--	--
3	1	Grating Exhaust-Unit 1	985	-482	14	10	16	1	1	-1	--	--
									2	-1	--	--
									3	-1	--	--
									4	-1	--	--
									5	-1	--	--
									6	1	3.25	33,000
4	1	Grating Intake-Unit 1	985	-436	14	10	16	1	1	-1	--	--
									2	-1	--	--
									3	-1	--	--
									4	-1	--	--
									5	-1	--	--
									6	1	3.25	33,000

TABLE II-1. TARGET LOCATION AND DESCRIPTION (Continued)

Target									Surface			
			Reference Point (ft)			Dimensions (ft)						
No.	Type	Description	X	Y	Z	WX	WY	WZ	No.	Mat'l	Thk (in)	Strength (psi)
5	1	Grating Exhaust-Unit 2	1005	-482	14	10	16	1	1	-1	--	--
									2	-1	--	--
									3	-1	--	--
									4	-1	--	--
									5	-1	--	--
									6	1	3.25	33,000
6	1	Grating Intake-Unit 2	1005	-436	14	10	16	1	1	-1	--	--
									2	-1	--	--
									3	-1	--	--
									4	-1	--	--
									5	-1	--	--
									6	1	3.25	33,000
7	2	Exhaust Stack Opening-Unit 1	990	-459	14	7	3.5	1	1	-1	--	--
									2	-1	--	--
									3	0	1	100
8	2	Exhaust Stack Opening-Unit 2	1010	-459	14	7	3.5	1	1	-1	--	--
									2	-1	--	--
									3	0	1	100
9	1	Diesel Oil Tank Compartment	962	-432	0	18	20	14	1	0	18	3,000
									2	0	18	3,000
									3	0	18	3,000
									4	0	18	3,000
									5	0	12	3,000
									6	-1	--	--

TABLE II-1. TARGET LOCATION AND DESCRIPTION (Continued)

Target									Surface			
			Reference Point (ft)			Dimensions (ft)						
No.	Type	Description	X	Y	Z	WX	WY	WZ	No.	Mat'l	Thk (in)	Strength (psi)
10	1	Airlock Structure	1420	-140	0	69	24	26	1	1	0.07	32,000
									2	1	0.07	32,000
									3	1	0.25	32,000
									4	1	0.07	32,000
									5	1	0.07	32,000
									6	-1	0	32,000
11	1	Turbine Building	1130	-288	0	138	270	66				
12	1	Inner Airlock Door-South Offset	1421	-159	-	1	18	21	1	1	0.25	32,000
									2	-1	--	--
									3	-1	--	--
									4	-1	--	--
									5	-1	--	--
									6	-1	--	--
13	1	Inner Airlock Door-North Offset	1421	-115	0	1	18	21	1	1	0.25	32,000
									2	-1	--	--
									3	-1	--	--
									4	-1	--	--
									5	-1	--	--
									6	-1	--	--
14	1	Office Building	1268	-244	0	38	226	36				
15	1	Reactor Building	1306	-162	0	114	144	96				
16	1	Maintenance Building	1120	36	0	136	124	30				

TABLE II-1. TARGET LOCATION AND DESCRIPTION (Continued)

Target								Surface			
			Reference Point (ft)			Dimensions (ft)					
No.	Type	Description	X	Y	Z	WX	WY	WZ	No.	Mat'l	Thk (in)	Strength (psi)
17	1	New Radwaste Building	1446	90	0	114	114	30				
18	1	Radwaste Building	1452	-98	0	152	64	39				
19	1	Machine Shop	1166	-368	0	104	80	1[4]				
20	1	Office Building	1280	-508	0	142	82	1[4]				
21	1	Storage Building	1110	-521	0	62	100	1[4]				
22	1	Guard House	1384	-338	0	58	58	1[4]				

Notes: [1] Target Type (T): 1 = Rectangular parallelepiped, 2 = circular cylinder.
[2] Surface No.: 1 = W wall, if target type (T) = 1; cylinder wall, if T = 2.
2 = S wall, if T = 1; cylinder top, if T = 2.
3 = E wall, if T = 1; cylinder base, if T = 2.
4 = N wall, if T = 1.
5 = Top, if T = 1.
6 = Base, if T = 1.
[3] Surface Material: 0 = Reinforced concrete, -1 = Imaginary, 1 = Steel.
[4] Since these buildings are assumed to fail, the structure height is nominally taken as 1 ft.

The diesel generator compartments and openings are modeled as the first 9 targets in Fig. II-1 and Table II-1. Target 1 is the Unit 1 compartment, which is constructed with 18-inch reinforced concrete walls (f_c' = 3000 psi) and a 12-inch reinforced concrete roof. The openings in the roof are modeled as Targets 3, 4, and 7. Targets 3 and 4 are the exhaust and intake grating sections, respectively. These heavy duty sections consist of 6 inch deep by 5/8 inch thick bridging plate sections on 1 3/16 inch centers with cross plates 1 inch deep by 3/8 inch thick on 4 inch centers. For the TORMIS perforation calculations, these sections are modeled as a solid plate with a depth of 3.25 inches, which gives the same mass per unit area as the grating. Target 7 is the 7 ft diameter exhaust stack opening and is modeled as an opening in which hit probabilities are scored with no penetration resistance. Thus, the stack itself is not modeled and the opening is modeled as a real surface to ensure TORMIS scoring of hit probability on the opening area. It is noted that the Diesel Generator Unit 2 compartment is the mirror image of Unit 1 compartment and is modeled by target numbers 2, 5, 6, and 8. From these combinations of targets, the diesel generator compartments are assumed to be damaged by tornado generated missiles if (1) the reinforced concrete walls or roof are scabbed, (2) the grating sections are perforated, or (3) the exhaust stack opening is hit by tornado generated missiles.

Target 9 is the Diesel Oil Tank Compartment. It is constructed of 3000 psi strength concrete with 18-inch walls and a 12-inch roof slab. Damage to this compartment is assumed to occur if the reinforced concrete is scabbed by a tornado generated missile.

The Airlock Structure is modeled as Target 10, which consists of the north and south walls, the roof, and the outer door. The steel plate outer door is 0.25 inches thick and has a yield strength of 32,000 psi. The wall

and roof sections are sandwich type construction consisting of metal siding 0.032 inches thick, an insulation layer, and an inner metal sheet 0.0478 inches thick. This twin wall construction has been reduced to a single sheet thickness for the TORMIS simulation. This calculation is based on the BRL perforation formula [13] and the Recht and Ipson residual velocity formula [2,14]. A single sheet thickness of 0.07 inches is used to model the Airlock wall and roof sections.

The Airlock Structure also has an inner door at the interface of the Reactor Building which can be closed to provide additional tornado missile protection. Since the current TORMIS methodology does not track missile trajectories once they have perforated an external target (such as Target 10), the additional protection provided by a closed inner door cannot be simulated. To provide approximate information on the probability of inner door perforation, Targets 12 and 13 were included in the plant model, as noted in Fig. II-1 and Table II-1. These targets simulate the presence of inner doors just to the north and south of the Airlock Structure. Since the Airlock Structure shields these targets from each other, the same missile cannot damage both Targets 12 and 13. This modeling technique allows estimation of inner door impact and perforation probabilities assuming that the Airlock Structure (Target 10) provides no resistance to tornado missiles. By summing the impact and damage probabilities for these two targets, one can conservatively estimate (from the same TORMIS simulation) the entrance probabilities to the Reactor Building corresponding to door-open and door-closed conditions.

The remaining structures in Fig. II-1 and Table II-1 are included in the plant model to reflect either shielding of the targets of interest or sources of missiles from atop structures or from the failure of nontornado proof

structures. Structures that are assumed to fail in severe winds include the Machine Shop (Target 19), Office Building (Target 20), Storage Building (Target 21) and Guard House (Target 22). Structures that are assumed to include some missile sources from cladding and roof equipment include the Turbine Building (Target 11), Reactor Building (Target 15), and both Radwaste Buildings (Targets 17 and 18).

B. Postulated Missile Threat

The missile threat that is postulated for the Airlock Structure and Diesel Generator Compartments includes buildings, loose objects, construction materials, vehicles and other sources over the plant site area. The missile characteristics are identical to those postulated in Ref. 1 for the cable tray bridge structures; thus, all potential missiles are categorized as one of the standard NRC missiles [15]. Additional structure origin missiles have been postulated for this study because the new targets of interest are located at plant grade elevations. As noted in Fig. II-2, a total of 14 areas were used to identify different missile origin zones.[1] The zones include storage and laydown areas, parking, switchyard, and adjacent open regions. These areas include the contiguous land region within the plant protected area and extends to about 1000 ft from the center of the plant. It is noted that previous simulations of missile trajectories and field observations suggest that the greatest hazard is from potential missiles that originate within several hundred feet of the target.

The numbers of each of the standard missile types [15] postulated by zone is summarized in Table II-2. A total of 13,855 potential missiles were specified to simulate the missile sources within these contiguous zones. This

---

[1] Zone 9 used in Ref. 1 has been subdivided to form a new Zone 9 and Zone 14. This subdivision was made to facilitate improved missile sampling in the vicinity of the diesel generator compartments.

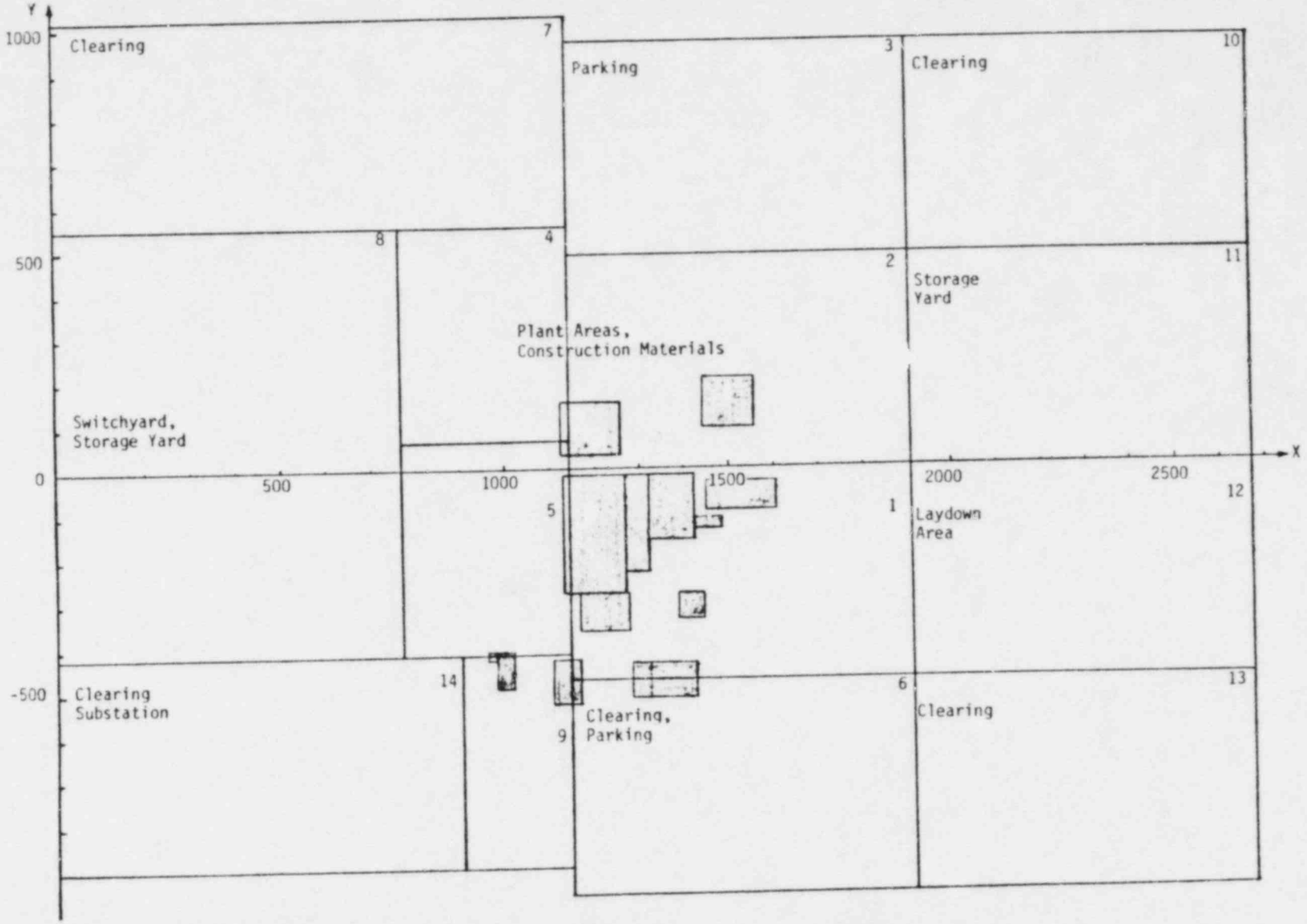

Figure II-2. Potential Missile Origin Zones

TABLE II-2. MISSILE SPECIFICATION BY ZONE

Missile Origin Zone	Number of Missiles By Type						
	1-in Rod	3-in Pipe	6-in Pipe	12-in Pipe	Wood Plank	Auto	Totals
1	200	200	200	200	200	100	1,100
2	500	500	500	500	500	50	2,550
3	100	100	100	100	100	250	750
4	100	100	100	100	100	250	750
5	100	100	100	100	100	20	520
6	100	100	50	50	250	100	650
7	10	10	10	10	10	10	60
8	200	200	200	200	200	10	1,010
9	90	90	9	9	90	5	293
10	10	10	10	10	100	10	150
11	200	200	200	200	200	10	1,010
12	200	200	200	200	200	100	1,100
13	10	10	10	10	100	10	150
14	10	10	1	1	10	5	37
15 (Str. 11)	75	50	50	25	0	0	200
16 (Str. 15)	75	50	50	25	0	0	200
17 (Str. 17)	75	50	50	25	0	0	200
18 (Str. 18)	75	50	50	25	0	0	200
19 (Str. 19)	175	150	150	125	100	0	700
20 (Str. 20)	200	150	50	0	300	0	700
21 (Str. 21)	400	300	100	0	600	0	1,400
22 (Str. 22)	50	25	25	0	25	0	125
Totals	2,955	2,655	2,215	1,915	3,185	930	13,855

missile population is identical to that given in Ref. 1 with the addition of the building failure missiles for structures 18, 19, 20, 21, and 22. These buildings are assumed to produce up to about 3,125 additional missiles that would originate near grade level in the vicinity of the diesel generator and airlock targets. These missiles are all conservatively assumed to be in the minimally restrained N' population, as described in Ref. 2. These missiles are specified to originate at heights that simulate storage characteristics above grade and missiles originating due to failure of nontornado-proof structural elements. The zone elevation and maximum injection heights are given in Table II-3. The minimum injection height of zone-origin missiles was conservatively considered to be five feet above the zone grade elevation; structure-origin missiles were injected at elevations characteristics of the structures themselves. The missiles were uniformly injected over the interval defined by these minimum and maximum heights. The automobile was injected between five and ten feet above grade for all zones.

C. Tornado Hazard

The input data for the tornado hazard definition was taken from an analysis of 19,085 tornado data entries reported in the 1950-1978 NSSFC data base [16]. Specifically, the data for tornado Region C in Ref. 8 was used in the specification of tornado intensity, path width, path length, and tornado direction. The design basis tornado with a windspeed of 360 mph [17] was used as the maximum intensity event. The angular difference of 15 degrees clockwise between plant north and true north was also accounted for in the directional tornado data input relative to the plant target model and missile zone geometry. These inputs are identical to those used in the Ref. 1 study.

TABLE II-3. MISSILE INJECTION HEIGHT BY ZONE

Missile Origin Zone	Injection Height Interval	Injection Height (ft) Above Grade					
		1-in Rod	3-in Pipe	6-in Pipe	12-in Pipe	Wood Plank	Auto
1,2,4,5,11,12	Min	5	5	5	5	5	5
	Max	25	25	25	25	25	10
3,6,7,10,13	Min	5	5	5	5	5	5
	Max	10	10	10	10	10	10
8,9,14	Min	5	5	5	5	5	5
	Max	40	40	40	40	40	10
15	Min	71	71	71	71	-	-
	Max	88	88	88	88	-	-
16	Min	101	101	101	101	-	-
	Max	124	124	124	124	-	-
17	Min	35	35	35	35	-	-
	Max	50	50	50	50	-	-
18	Min	40	40	40	40	-	-
	Max	53	53	53	53	-	-
20,21,22	Min	1	1	1	1	1	-
	Max	15	15	15	15	15	-
19	Min	1	1	1	1	1	-
	Max	30	30	30	30	30	-

III. RESULTS

A. Tornado Windspeed Exceedance Probabilities

The tornado windspeed curve developed in Ref. 1 is based on a regional evaluation of the tornado windspeeds at Oyster Creek. The developed windspeed vs probability of exceedance curve is considered to be a conservative estimation of tornado wind probabilities at Oyster Creek as a result of: (1) the use of conservative F-scale windspeed transformations [cf. Ref. 6]; (2) the use of a 360 mph upperbound tornado intensity windspeed; (3) the use of mean regional occurrence rates as opposed to site-specific data (for example, see maps in Ref. 18); and (4) the calculation of windspeed exceedance probabilities for an elevation of 62 feet above grade (which corresponds to the elevation of the cable tray bridges). The developed curve is repeated as Fig. III-1; a second curve is shown to reflect the windspeed adjustment to elevation 33 ft above grade (standard anemometer height). This adjustment is less than about 15 mph at all exceedance probabilities and is based on tornado wind profile variation with height above ground [2]. It is noted that a site-specific evaluation of tornado windspeed risk for the Oyster Creek Station would probably result in a substantial shift in the windspeed curve. For example, we would expect the 10^{-6} windspeed to be less than 200 mph, based on information in Ref. 12 for average Region C windspeed risks.

B. Tornado Missile Impact and Damage Probabilities

Missile impact and damage probabilities to the Airlock Structure and Diesel Generator Structures have been estimated using the TORMIS computer code simulation methodology. The TORMIS input data set was developed from information in Section II and Ref. 1. Initial simulations of about 5,000 missile histories were made to check the plant, missile, and simulation parameter inputs. At the completion of this checking phase the production run

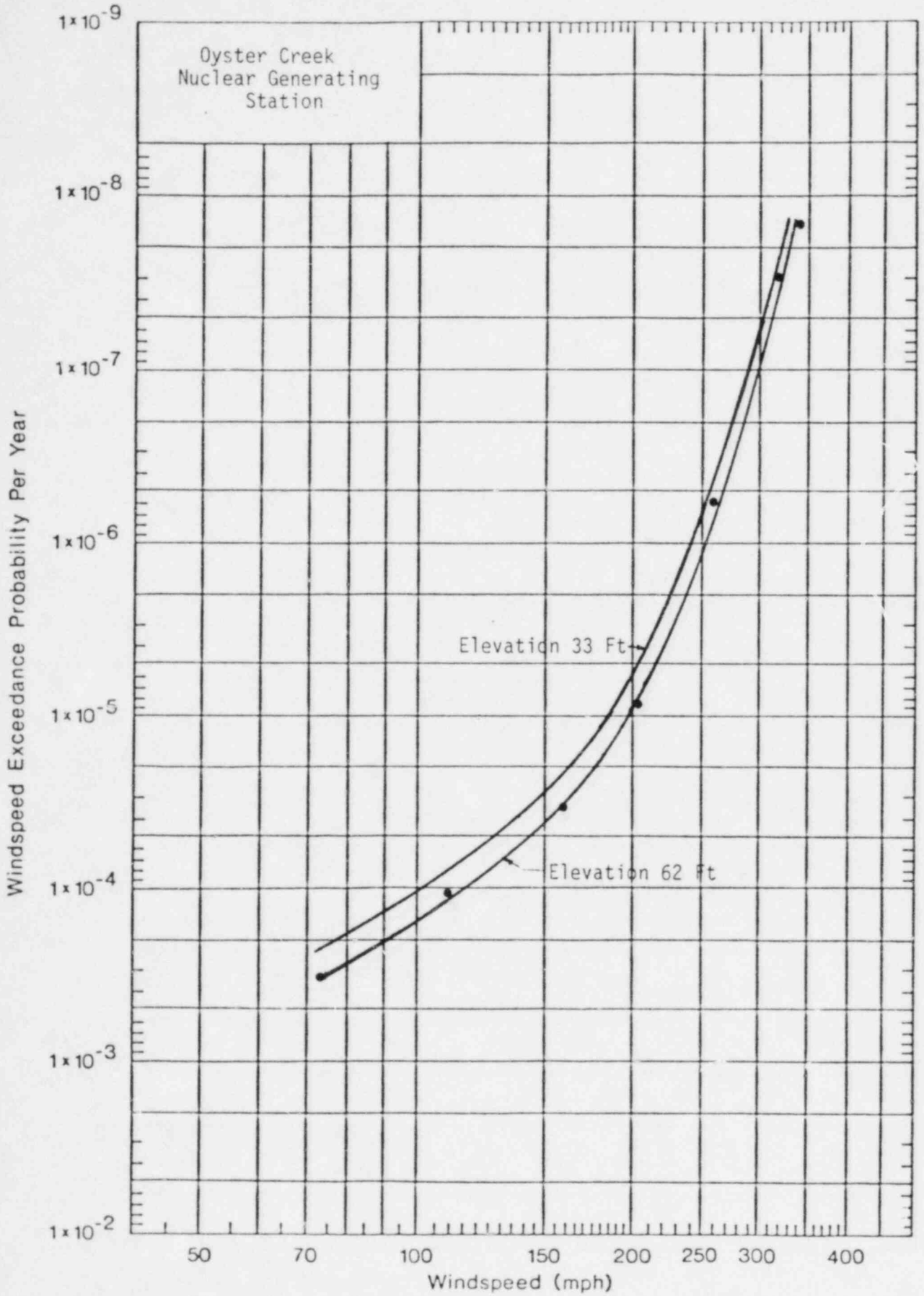

Figure III-1. Tornado Windspeed Exceedance Probabilities

simulations were submitted in two separate batches. Each batch consisted of a total of 30,000 tornado missile histories, corresponding to 5,000 histories for each F-scale intensity from F'1 through F'6. The variance reduction parameters were developed separately for the Diesel Generator targets (Batch 1) and the Airlock Structure targets (Batch 2). This procedure follows the recommended TORMIS approach for separate target clusters, as outlined in Ref. 2. The results of these F-scale simulations were aggregated to yield total probability estimates over all tornado intensities for each diesel generator and airlock structure target.

The results of the TORMIS simulations are summarized in Table III-1. These results are reported separately for penetrator missiles (1-in rod, 3-in pipe, 6-in pipe, 12-in pipe, and wood plank) and the vehicle missiles. Impacts for vehicles are scored separately in TORMIS because their impact characteristics and induced structural mode of response are different from the penetration type missiles. Impact probabilities for the vehicles are determined, and the probabilities of impact with velocities greater than specified velocities are also estimated in the TORMIS methodology. This information can then be used as needed in design safety-checking for overall structural response analysis. If the results of such an analysis indicate that the vehicle contributes to the damage risk, then this risk is combined with the penetration damage missile probabilities.

1. Diesel Generator Targets

For the diesel generator targets, penetrator missile impacts were obtained for all 9 targets. The missile hit probability is estimated as 4.6×10^{-5} and 5.4×10^{-6} per year for Targets 1 and 2, respectively. The increased hit probability of Target 1 over Target 2 is due principally to the

TABLE III-1. TARGET IMPACT AND PERFORATION PROBABILITIES

		Penetrator Missiles						Automobile Missiles V_i > 57 mph					
		Impact			Scabbing, Perforation Damage			Impact					
Target Number	Target Description	Lower Bound	Mean	Upper Bound	Lower Bound	Mean	Upper Bound	Lower Bound	Mean	Upper Bound	Lower Bound	Mean	Upper Bound
1	DG-U1	1.3 E-5	4.6 E-5	7.9 E-5		*		0	9.4 E-7	2.5 E-6	0	7.9 E-10	1.7 E-9
2	DG-U2	3.0 E-7	5.4 E-6	1.1 E-5		*		0	2.9 E-7	6.9 E-6	0	1.8 E-8	4.2 E-8
3	GE-U1	0	1.5 E-9	4.4 E-9		*			*			*	
4	GI-U1	0	9.9 E-9	2.8 E-8		*			*			*	
5	GE-U2	0	1.8 E-9	5.3 E-9		*			*			*	
6	GI-U2	0	9.3 E-9	2.7 E-8		*			*			*	
7	ESO-U1	0	1.1 E-7	3.1 E-7	0	1.1 E-7	3.1 E-7		*			*	
8	ESO-U2	0	4.8 E-9	1.4 E-8	0	4.8 E-9	1.4 E-8	0	1.7 E-9	4.9 E-9	0	1.7 E-9	4.9 E-9
9	DOTC	2.3 E-7	5.1 E-6	9.9 E-6		*		0	1.5 E-8	4.0 E-8		*	
10	AS	5.4 E-6	1.4 E-5	2.3 E-5	4.2 E-7	6.6 E-6	1.3 E-5	0	1.0 E-6	2.7 E-6	0	1.0 E-6	2.7 E-6
12	IAD-SO		*			*			*			*	
13	IAD-NO	0	1.1 E-6	2.5 E-6		*		0	2.0 E-8	5.9 E-8	0	2.0 E-8	5.9 E-8
3∩5			*			*			*			*	
3∪5		0	3.3 E-9	7.8 E-9		*			*			*	

* Denotes no impacts or damages occurred in the simulations.

south and west wall exposures of Target 1. Neither diesel generator compartment was scabbed on the 18-in reinforced concrete walls or the 12-inch roof barriers, as noted in Table III-1.

The impact probability on the diesel oil tank compartment is estimated at about 5.07×10^{-6} per year. No scabbing damages occurred in the TORMIS simulations on the 18-inch reinforced concrete walls. Hence, the 18-inch walls and 12-inch roof slabs are not vulnerable to penetrator-type tornado missile damage. In addition, the vehicle missile impact probability for impact speeds greater than 57 mph is less than 10^{-7} per year for the diesel generator targets.

The probability of hitting the exhaust grating targets was estimated as 1.5×10^{-9} and 1.8×10^{-9} for Units 1 and 2, respectively. The hit probability for the intake gratings is about 9×10^{-9} for both units. These small probabilities and the variation for similar size targets reflect the rooftop location of these targets and their relatively small size (160 sq ft). For missiles originating near grade to impact these roof targets, they must be lifted up by the winds and dropped onto the gratings, which have no exposure in the vertical direction. As noted in Table III-1, these heavy duty gratings were not perforated in any of the TORMIS simulations. Hence, we conclude that the grating perforation probability is negligible.

Targets 7 and 8 represent the Exhaust Stack openings for compartments 1 and 2, respectively. These targets were modeled with no perforation resistance and hence missile impact is assumed to be equivalent to missile entrance into the diesel generator compartment. These missile entrance probabilities vary from 1.1×10^{-7} for Target 7 to 4.8×10^{-9} for Target 8. The variation in impact probability is due to statistical imprecision because so few histories resulted in impacts on these rooftop targets.

Based on the variation in results for the diesel-generator rooftop targets, a smoothing technique is used to obtain best-estimate missile entrance probabilities to the exhaust stack openings. Averaging the missile hit probability per unit area for Targets 3 through 8, one obtains a missile hit probability (including automobile impact) of 5×10^{-10} per sq ft. Hence, the smoothed best-estimate missile entrance probability through an Exhaust Stack opening of 39 sq ft is 2×10^{-8} per year. Considering the statistical uncertainties from the simulation sample size (which introduces a factor of about 2.5 at tne 95 percent confidence level) and a modeling uncertainty factor of about 2, a conservative estimate of the probability of missile entrance to a single compartment would be $(2 \times 10^{-8}) \times (2.5) \times (2) = 1.0 \times 10^{-7}$ per year. Since the reinforced concrete walls and heavy duty grating sections are not vulnerable to tornado missile damage, this probability constitutes the primary tornado missile risk contribution to the Diesel Generator compartments.

2. Airlock Structure

The estimated impact and perforation probabilities for the Airlock Structure are 1.4×10^{-5} and 6.6×10^{-6} per year, respectively. These probabilities indicate that the conditional perforation probability given missile impact is about 0.5 for this target. This relatively high conditional perforation probability is consistent with the thin gage side and roof deck on this structure. The 95 percent upperbound confidence level on the mean perforation probability is about 1.3×10^{-5} per year. The estimated probability of automobile impact with $V_i > 57$ mph is about 1×10^{-6} per year.

The Airlock Structure is located on the east side of the Reactor Building and is oriented in an east-west direction. Hence, the main exposure of this target are its north and south walls and roof deck. Since the majority of

tornadoes approach from the west and southwest direction in this region [cf. Ref. 2], the most severe threat to this structure occurs from missile transport from the southwest and south directions. These missiles will impact the Airlock Structure with a velocity vector parallel to or directed away from the east wall of the Reactor Building. Missiles that originate on the north side of the Airlock Structure pose a threat to Target 10 if they are also on the weak side of the tornado. These missiles will tend to impact the Airlock Structure with a velocity vector directed towards the Reactor Building. However, since this side is shadowed by Targets 15 and 18, the number of potential missiles are fewer and the missile acceleration distance is shorter. Thus, considering directional tendencies of tornadoes, the orientation of the Airlock Structure, and the presence of adjacent buildings, it seems unlikely that perforation of the Airlock would necessarily result in missile entrance to the Reactor Building. It is our opinion that the frequency of missile entrance to the Reactor Building given Airlock Structure perforation is less than 0.5 and probably on the order of about 0.2, based on tornado directional tendencies[1] and the Oyster Creek Station layout. Thus, a conservative estimate of the Reactor Building missile entrance probability is about $(1.3 \times 10^{-5}) \times (0.5) = 6 \times 10^{-6}$ per year.

The missile perforation and entrance probabilities discussed above for the Airlock Structure do not take into account the presence of the 1/4-inch steel plate inner door. It was thus assumed that the inner door is open during the tornado strike. To provide additional insight regarding the importance of the inner door and the role of shadowing and east-west orientation of the Airlock Structure, two additional targets were modeled in

---

1 Only 20 percent of tornado paths are from directions other than west or southwest.

the TORMIS simulations. As discussed previously, these are Targets 12 and 13 in Fig. II-1 and Table II-1. These targets simulate the plate thickness and size of the Airlock inner door. They were positioned on either side of the Airlock Structure to account for shadowing provided by the Airlock and to estimate the probabilities of impact and damage to a rather small target on the east side of the Reactor Building. The results in Table II-1 indicate that no impacts were obtained on Target 12 and that no perforations were obtained on Target 13. The impact probability on Target 13 was estimated at about 1.1×10^{-6} per year, which about 20 percent of the above conservative estimates of the Reactor Building entrance probability of 6×10^{-6} per year.

These results for Targets 12 and 13 tend to confirm the missile trajectory patterns previously discussed and observed in other tornado missile analyses [2]. That is, Target 12 is on the east side of the Reactor Building and is shadowed by Target 10 to the north. Hence, the primary mechanism through which missiles impact Target 12 is through east-west or southeast-northwest missile transport. This transport is highly unlikely in cyclonic windfields whose principal translational direction is toward the northeast and east sectors. The directed peak wind vectors are in the north and northeast sector on the right hand side and in the west-south sector on the left hand side of the tornado center. Since Target 12 is protected by Target 10 in this simulation, the lack of impacts in the TORMIS simulation is not surprising. Thus, the main threat to an opening on the east side of the Reactor Building is for missiles positioned on the weak side of the tornado which would be accelerated into the southeast quadrant. From Fig. II-1, we note that the number of missiles and runup distance is quite limited due to the presence of Target 18. Hence, it is also not unusual that Target 13 was hit but not perforated in the TORMIS simulation.

C. Missile Impact Velocities on Diesel Generator Roof Panels

The tornado missile simulations in the TORMIS methodology provide estimates of: (1) the probability of missiles impacting the plant structures and (2) the probability of local damage to the structures. The local damage calculations are made using penetration, scabbing, and perforations formulas that have been updated on the basis of tornado missile impact tests on reinforced concrete barriers. References 2, 4, and 9 describe the models used for the local effects damage calculations. The TORMIS methodology does not explicitly evaluate other failure modes, such as overall dynamic response. As noted in Refs. 2 and 4, these failure modes are not dominant for most tornado missile impact on rigidly built reinforced concrete structures at nuclear power plants. However, the TORMIS printout includes an output data stream that can be used to quantify missile impact characteristics for such calculations.

1. Model for Missile Velocity Distribution

The roof panels on the diesel generator compartments at Oyster Creek are made of removable concrete panels with support provided by structural steel channel sections. Questions have been raised regarding the adequacy of these roof structures to withstand impacts by missiles that might induce a failure other than scabbing or perforation of the concrete panels. The TORMIS output has been reviewed to estimate the velocity characteristics of missiles that were predicted to impact the roof of a diesel generator compartment. When this velocity distribution is coupled with the roof impact probability, one can estimate the probability of tornado-generated missiles impacting the roof panels at different speeds. The TORMIS output provides estimates of

$f(v|H)$, the velocity distribution given roof impact, and $p^N(H)$, the multiple missile roof impact probability. With this data, one obtains the conditional missile velocity exceedance probability from

$$P(v > V^*|H) = 1 - \int_0^{V^*} f(v|H)dv \qquad (1)$$

and the total probability from

$$P(v > V^*) = P(v > V^*|H)\ p^N(H) \quad . \qquad (2)$$

2. Missile Velocity Functions

As noted on p. III-6, $p^N(H)$ is estimated as 5×10^{-10} per sq ft for the diesel generator roof. The roof area is 20 ft x 78 ft and thus $p^N(H) = 7.8\times10^{-7}$ per year. A review of the TORMIS output indicates that a total of 8 missile impacts occurred on the diesel generator roof area. These impact velocities V_i ranged from 49 to 105 ft/sec. Most of these impacts correspond to highly oblique velocity vectors that result from horizontally accelerated missiles hitting an elevated horizontal surface. The TORMIS methodology accounts for these oblique and non-collinear impacts by computing an effective normal velocity V_i' for each missile impact [cf. 2]. The range of effective velocity for these eight impacts is from 6.5 to 38.4 ft/sec. Fig. III-2 is a plot of the V_i and V_i' distributions on log-normal probability paper. The near linear plots are judged to provide reasonable models of $P(v > V^*|H)$ for the diesel generator roof panels.

A plot of the total probability $P(v > V^*)$ is given in Fig. III-3 for both V_i and V_i'. The 10^{-7} exceedance probability speeds are about 35 ft/sec for V_i' and 110 ft/sec for V_i. Since this calculation is based on all missile types and the speeds are dominated by the lighter missiles, Fig. III-3 should be conservative for heavier missiles of interest in an overall response

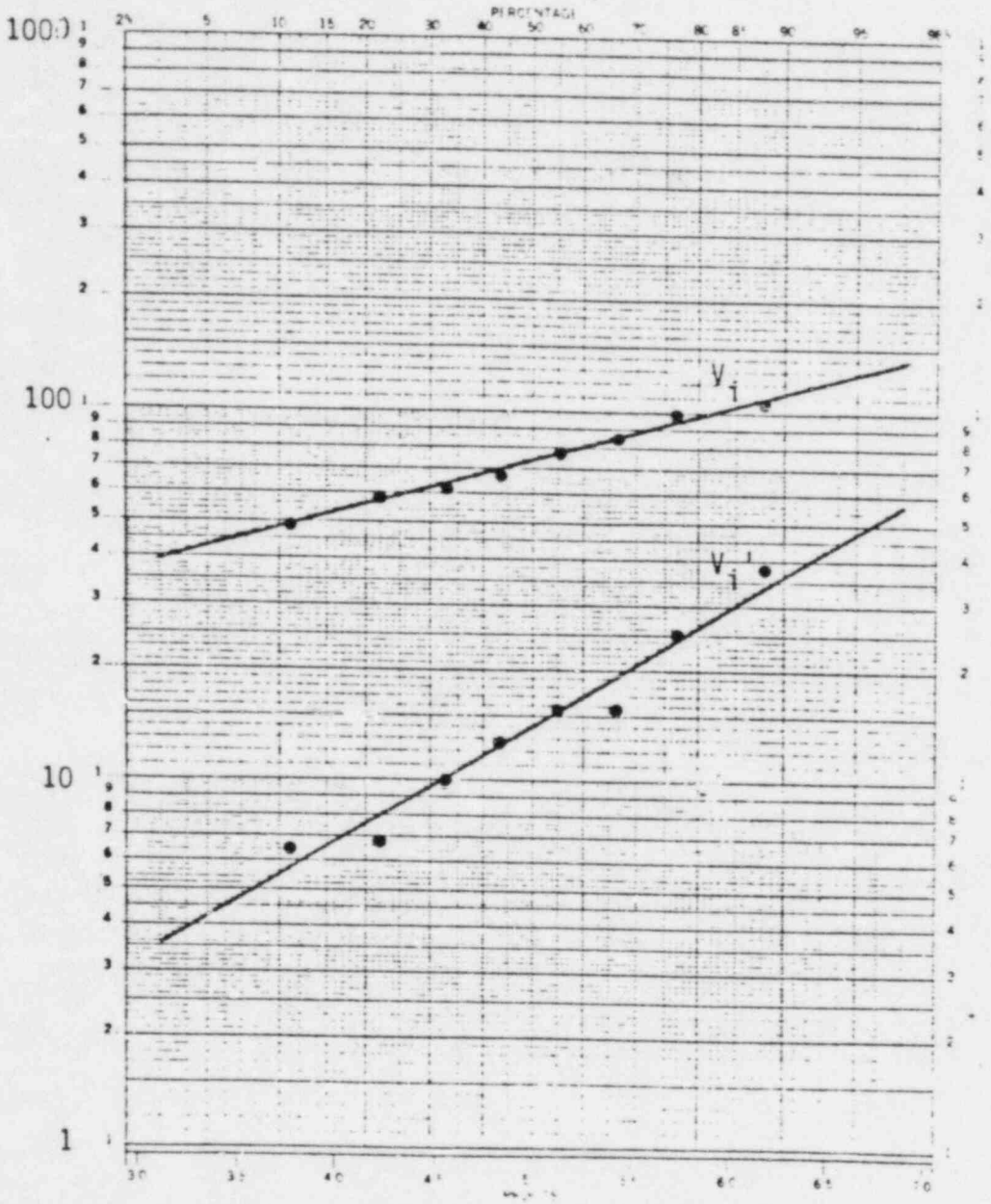

Figure III-2. Impact Velocity Probability Distributions

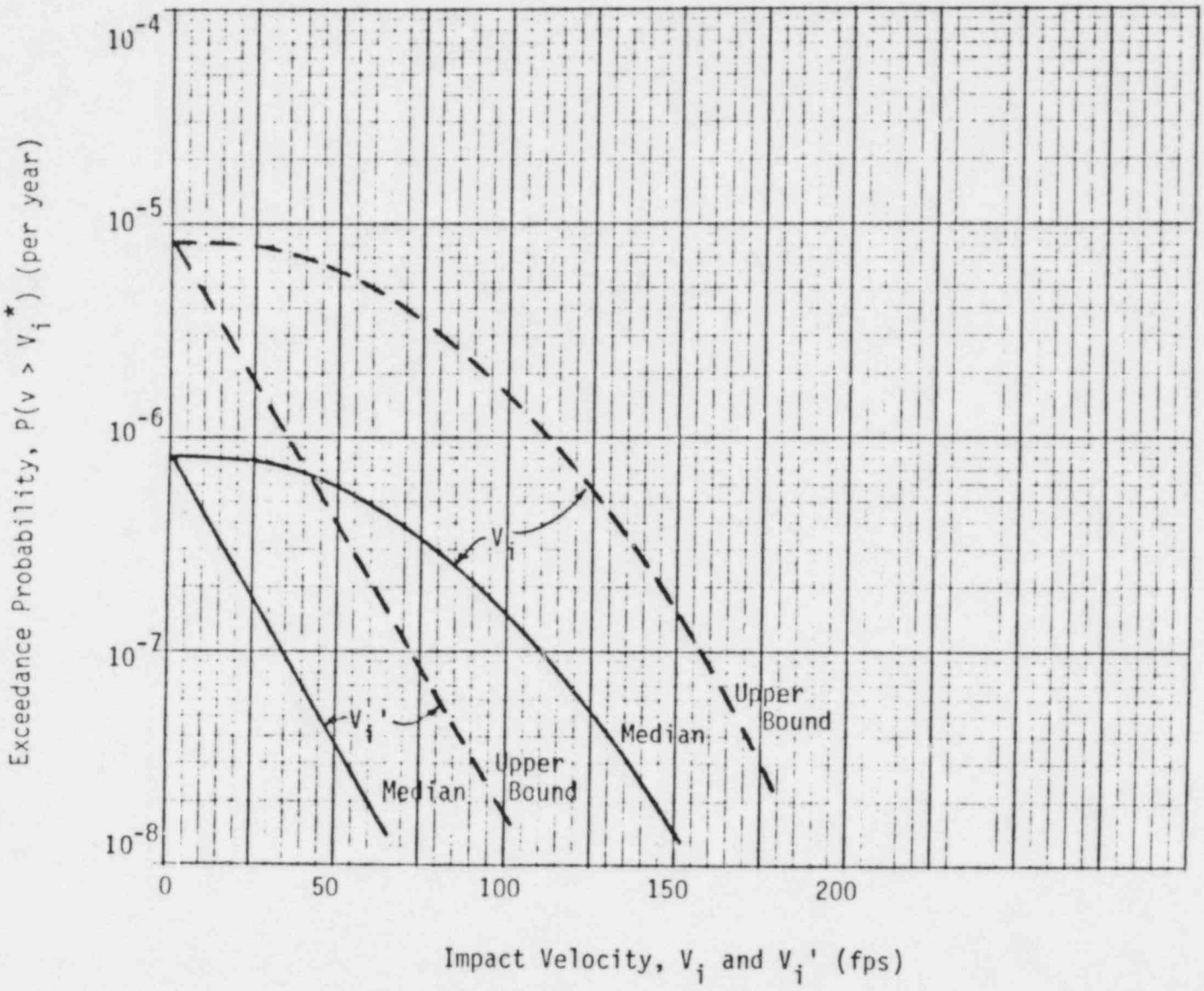

Figure III-3. Diesel Generator Roof Impact Velocity Probabilities

failure mode calculation. A second point in the use of these data is that for a conservatively oriented calculation, the results snould be adjusted for statistical sampling and model uncertainties. The statistical and model uncertainties are estimated to introduce a factor of 5 uncertainty in the $p^N(H)$ calculation (see page III-6). We introduce an additional factor of 2 for the $P(v > V^*|H)$ estimation and thus recommend a factor of 10 as representative of the uncertainty in $P(v > V^*)$ for a conservative calculation. Thus, the dashed curves for V_i and V_i' in Fig. III-3 should be used to select the appropriate V_i or V_i' for a conservative calculation. Following this procedure, conservative 10^{-7} values of V_i and V_i'correspond to about 160 and 75 ft/sec, respectively. It is noted that V_i' velocities are appropriate for loads acting normal to the roof panels.

IV. CONCLUSIONS

Based on the results of 60,000 tornado missile simulations using the TORMIS methodology, we make the following conclusions for the Oyster Creek station:

1. Diesel Generator Compartments. The probability of tornado missile damage to a single diesel generator compartment is less than about 1×10^{-7} per year. This probability is dominated by missile entrance through the 7 ft exhaust stack opening on top of the compartment. No damages to the reinforced concrete walls and roof of either diesel compartment, or to the diesel oil tank compartment, or to the heavy duty gratings were obtained in the TORMIS simulations.

2. Airlock Structure - Open Inner Door. The missile entrance probability for the Airlock Structure is estimated as 6.6×10^{-6} per year with the 95 percent confidence limit on the mean probability estimated as 1.0×10^{-5} per year. Considering the probability of missile entrance given Airlock perforation, we estimate the missile entrance probability through an open inner-door to be within a range of about 1×10^{-6} to 6×10^{-6} per year.

3. Airlock Structure - Closed Inner Door. If the inner Airlock door is closed a fraction of the time, p, a conservative estimate of the missile entrance probability to the reactor building through the Airlock area is (1-p)·(Airlock perforation probability) per year. For example, if p is 0.8, then an estimate of the range of missile entrance probability is about 2×10^{-7} to 1×10^{-6} per year.

These probabilities are based on numerical estimates obtained from a plant-specific evaluation with judgemental factors and some consideration of statistical and model uncertainties. It is noted that the confidence intervals on the mean probabilities given in Table III-1 include only the statistical uncertainties resulting from a finite sample size in the Monte Carlo calculations. In the absence of additional simulations and sensitivity analyses using a more general missile spectrum, these probabilities constitute our best estimate for Oyster Creek. They reflect statistical and model uncertainties as well as conservatisms in the tornado parameters, number of missiles, and TORMIS missile injection methodology.

V. REFERENCES

1. Twisdale, L. A., and Dunn, W. L., "Tornado Windspeed and Missile Risk Analysis of Cable Tray Bridges at Oyster Creek Nuclear Generating Station," Final Report 44T-2382, Prepared for Pickard, Lowe and Garrick, Inc., Research Triangle Institute, Research Triangle Park, North Carolina, April 1982.

2. Twisdale, L. A., and Dunn, W. L., "Tornado Missile Simulation NP-440, and Design Methodology," EPRI NP-2005, Electric Power Research Institute, Palo Alto, California, August 1981.

3. Markee, E. H., Beckerley, J. G., and Sanders, K. E., "Technical Basis for Interim Regional Tornado Criteria," WASH-1300, 1974.

4. Twisdale, L. A., et al, "Tornado Missile Risk Analysis," EPRI NP-768 (Vol. I) and EPRI NP-769 (Vol. II), Electric Power Research Institute, Palo Alto, California, May 1978.

5. Twisdale, L. A., "Risk-Based Design Against Tornado Missiles," Proceedings of the Third ASCE Specialty Conference on Structural Design of Nuclear Power Plant Facilities, Boston, Massachusetts, April 1979.

6. Twisdale, L. A., "Tornado Data Characterization and Windspeed Risk," Journal of the Structural Division, Proceedings ASCE, Vol. 104, No. ST10, October 1978.

7. Twisdale, L. A., Dunn, W. L., and Davis, T. L., "Tornado Missile Transport Analysis," Journal of Nuclear Engineering and Design, 51, 1979.

8. Dunn, W. L., and Twisdale, L. A., "A Synthesized Windfield Model for Tornado Missile Transport," Journal of Nuclear Engineering and Design, 52, 1979.

9. Twisdale, L. A., "Probabilistic Considerations in Missile Impact Assessment," Proceedings of the International Seminar on Probabilistic Design of Nuclear Power Plants, San Francisco, California, August 1977.

10. Twisdale, L. A., "An Assessment of Tornado Windfield Characteristics for Missile Loading Prediction," Proceedings of the Fourth U.S. National Conference on Wind Engineering Research, University of Washington, Seattle, Washington, July 1982.

11. Twisdale, L. A., "Regional Tornado Data Base and Error Analysis," Preprint, AMS Twelfth Conference on Severe Local Storms, San Antonio, Texas, January 1982.

12. Twisdale, L. A., and Dunn, W. L., "Probabilistic Analysis of Tornado Wind Risks," Journal of Structural Engineering, Vol. 109, No. 2, February 1983.

13. Gwaltney, R. C., "Missile Generation and Protection in Light-Water-Cooled Power Reactor Plants," USAEC Report ORNL-NSIC-22, Oak Ridge National Laboratory, September 1968.

14. Recht, R. F., "Ballistic Perforation Dynamics," Journal of Applied Mechanics, Trans. ASME, 30, 386, 1963.

15. Nuclear Regulatory Commission, "Missiles Generated by Natural Phenomena," Section 3.5.1.4, Standard Review Plan, Revision 1, November 1975.

16. Kelly, D. L., et al., "An Augmented Tornado Climatology," Monthly Weather Review, Vol. 106, August 1978, pp. 1172-1183.

17. Nuclear Regulatory Commission, "Design Basis Tornado for Nuclear Power Plants," Regulatory Guide 1.76, April 1974.

18. Fujita, T. T., "Workbook of Tornadoes and High Winds," SMRP Research Paper 165, Department of Geophysical Sciences, University of Chicago, Chicago, Illinois, 1978.

5. TORNADO MISSILE CONSEQUENCE ANALYSIS

The loss of offsite AC power (LOOP) plant model for Oyster Creek developed in Reference 2 was used to evaluate the consequences (in terms of impact on core melt frequency) for each of the two tornado missile scenarios summarized in Section 3 and defined in detail in Section 4 of this report. The loss of offsite AC power event sequence diagram and event tree are reproduced here as Figures 5-1 and 5-2, respectively. In order to evaluate the core melt frequency contribution or impact, the following quantification process was utilized:

[Initiating Event Frequency For Tornado Missile Induced Loss of Offsite AC Power and Plant Damage

Scenario 1 = 1.0×10^{-7}/year

Scenario 2 = 6.0×10^{-6}/year] x [Conditional Electric Power State Frequency] x [Conditional Frequency of Plant Damage State Given Electric Power State and Initiating Event Scenario (using loss of offsite AC power event tree)] = Core Melt Frequency Contribution

The input data tables and output results are shown in Tables 5-1 through 5-4 for Scenario 1 and Tables 5-5 through 5-8 for Scenario 2. Scenario 1 which is assumed to disable both diesel generators only affects the electric power state frequencies in Table 5-1 giving the results in Table 5-2. The loss of offsite AC power quantification using the input data in Table 5-3 remains unchanged from Reference 2 except for the initiating event/electric power state frequency. Scenario 2 is assumed to fail (with a conditional frequency of 1.0) all the top events in the loss of offsite AC power event tree except for Events E1, E2, E4, E5, E6a, and E7 which remain unchanged from Reference 2. The electric power state frequency quantification is the same as the loss of offsite AC power case in Reference 2. The resultant core melt frequencies are shown in Tables 5-4 and 5-8 and reproduced below:

Scenario 1: 1.0×10^{-11} per reactor year

Scenario 2: 1.4×10^{-7} per reactor year

TABLE 5-1. TORNADO MISSILE SCENARIO 1 ELECTRIC POWER EVENT TREE INPUT DATA

Electric Power Top Event	Conditional Frequency of Failure		Data Source (Reference 3)
	Mean	Variance	
EP - Demand for Electric Power	1.0	N/A	N/A
DB - DC Center B Available	3.79-4	1.42-8	Page A-82 (numbers 1 through 4)
DC - DC Center C Available	3.79-4	1.42-8	Page A-82 (numbers 1 through 4)
OP - Offsite AC Power Available to Both Startup Transformers	1.0	N/A	Tornado Missile Causes Loss of Offsite Power
OA - Offsite AC Power Transferred to Buses 1A and 1C (S1A circuit breaker closes)	N/A	N/A	N/A
OB - Offsite AC Power Transferred to Buses 1B and 1D (S1B circuit breaker closes)	N/A	N/A	N/A
D1 - Diesel Generator 1 Supplies AC Power to Bus 1C	1.0	N/A	Tornado Missile Disables Diesel Generator
D2 - Diesel Generator 2 Supplies AC Power to Bus 1D	1.0	N/A	Tornado Missile Disables Diesel Generator

NOTE: Exponential notation is indicated in abbreviated form; i.e., 3.79-4 = 3.79×10^{-4}.

TABLE 5-2. TORNADO MISSILE SCENARIO 1 CONDITIONAL ELECTRIC POWER STATE FREQUENCIES

Electric Power State	Initiating Event Category
	Loss of Offsite Power (T4) Due to Tornado Missile
EP-1 (2 AC-Offsite, 2 DC)	0.0
EP-2 (2 AC-Diesel Generators, 2 DC)	0.0
EP-3 (1 AC-Offsite, 1 DC)	0.0
EP-4 (1 AC-Diesel Generators, 1 DC)	0.0
EP-5A (No AC, 2 DC)	1.0
EP-5B (No AC, No DC)	7.58-4

NOTE: Exponential notation is indicated in abbreviated form; i.e., 7.58-4 = 7.58×10^{-4}.

TABLE 5-3. LOSS OF OFFSITE POWER (T4) DUE TO TORNADO MISSILE SCENARIO 1
EVENT TREE INPUT DATA

Event Tree Top Event Description	Electric Power States Conditional Frequency of Failure (mean)						Data Source (Reference 2 if Section Number, Reference 3 if Page Number)
	EP-1 2 AC (offsite) 2 DC 0.0	EP-2 2 AC (DG's) 2 DC 0.0	EP-3 1 AC (offsite) 1 DC 0.0	EP-4 1 AC (DG) 1 DC 0.0	EP-5A No AC 2 DC 1.0	EP-5B No AC No DC 7.58-4	
T4 - Loss of offsite Power (1.00-7)	0.0	0.0	0.0	0.0	1.00-7	7.58-11	Product of IE and EP Frequency
RS - Reactor Scram	5.40-5	5.40-5	5.40-5	5.40-5	5.40-5	5.40-5	Page A-102
IV - MSIVs Close	5.28-4	5.28-4	5.28-4	5.28-4	5.28-4	5.28-4	Section B.5
BV - Turbine Control System Closes By-pass Valves	3.67-2	3.67-2	3.67-2	3.67-2	3.67-2	3.67-2	Page A-458 and Section B.2
PR - Pressure Relief, EMRVs or Safety Valves Open	$< 10^{-9}$	$< 10^{-9}$	$< 10^{-9}$	$< 10^{-9}$	$< 10^{-9}$	$< 10^{-9}$	Section B.9
CV - EMRVs or Safety Valves Close	1.79-2	1.79-2	1.79-2	1.79-2	1.79-2	5.50-5	Section B.9
IC - Isolation Condenser Actuation	1.19-5	8.36-6	3.45-3	2.90-3	8.36-6	5.00-2	Section B.7

NOTES:

1. Exponential notation is indicated in abbreviated form; i.e., 7.58-4 = 7.58×10^{-4}.
2. EP = electric power; DG = diesel generator; IE = initiating event.

TABLE 5-3 (continued)

Event Tree Top Event Description	Electric Power States Conditional Frequency of Failure (mean)						Data Source (Reference 2 if Section Number, Reference 3 if Page Number)
	EP-1 2 AC (offsite) 2 DC 0.0	EP-2 2 AC (DG's) 2 DC 0.0	EP-3 1 AC (offsite) 1 DC 0.0	EP-4 1 AC (DG) 1 DC 0.0	EP-5A No AC 2 DC 1.0	EP-5B No AC No DC 7.58-4	
MU - Isolation Condenser Shell Side Makeup	3.96-3	3.96-3	3.96-3	3.96-3	6.48-4	6.48-4	Page A-513
CR - Control Rod Drive Flow	2.00-3	2.00-3	7.00-3	7.00-3	1.0	1.0	Section B.8
VO - EMRVs or Safety Valves Open	$< 10^{-9}$	$< 10^{-9}$	$< 10^{-9}$	$< 10^{-9}$	$< 10^{-9}$	$< 10^{-9}$	Section B.9
AD - ADS Actuation	9.70-4	9.70-4	9.70-4	9.70-4	9.70-4	1.0	Section B.10
CS - Core Spray Injection	3.71-4	3.71-4	9.39-4	9.39-4	1.0	1.0	Section B.11
CC - Suppression Pool (containment) Cooling	3.75-3	3.75-3	3.75-3	3.75-3	1.0	1.0	Section B.12
CF - CRD Flow	2.00-3	2.00-3	7.00-3	7.00-3	1.0	1.0	Section B.8
FP - Fire Protection Water to Core Spray	5.25-4	5.25-4	5.25-4	5.25-4	5.25-4	5.25-4	Page A-368

NOTES:

1. Exponential notation is indicated in abbreviated form; i.e., 7.58-4 = 7.58×10^{-4}.
2. EP = electric power; DG = diesel generator; IE = initiating event.

TABLE 5-4. SUMMARY OF RESULTS EVENT TREE T4 (TORNADO MISSILE SCENARIO 1) QUANTIFICATION

Event Sequence State			Mean Frequency (events per reactor year)	Core Melt Frequency (events per reactor year)
Success State	Transfer States			
	To Another Event Tree	To Containment Event Tree		
S1			9.81-8	
S2			0.00	
S2/F			0.00	
S3			0.00	
S3/B			0.00	
S4/F			0.00	N/A
S4/FB			0.00	
S5/F			1.85-9	
S5/FB			1.93-12	
S6			0.00	
S6/B			0.00	
	L1		< 1.00-13	
		ELDF	9.73-13	
		ELDS	0.00	
		EHD-	3.90-12	1.0-11
		ELDFB	< 1.00-13	
		ELDSB	0.00	
		EHD-B	3.35-15	
		ATWS	5.40-12	

NOTE: Exponential notation is indicated in abbreviated form; i.e., 9.81-8 = 9.81×10^{-8}.

TABLE 5-5. TORNADO MISSILE SCENARIO 2 ELECTRIC POWER EVENT TREE INPUT DATA

Electric Power Top Event	Conditional Frequency of Failure		Data Source (Reference 3)
	Mean	Variance	
EP - Demand for Electric Power	1.0	N/A	N/A
DB - DC Center B Available	3.79-4	1.42-8	Page A-82 (numbers 1 through 4)
DC - DC Center C Available	3.79-4	1.42-8	Page A-82 (numbers 1 through 4)
OP - Offsite AC Power Available to Both Startup Transformers	1.0	N/A	Tornado Missile Causes Loss of Offsite Power
OA - Offsite AC Power Transferred to Buses 1A and 1C (S1A circuit breaker closes)	N/A	N/A	N/A
OB - Offsite AC Power Transferred to Buses 1B and 1D (S1B circuit breaker closes)	N/A	N/A	N/A
D1 - Diesel Generator 1 Supplies AC Power to Bus 1C	5.44-2	1.59-4	Page A-84 (numbers 23 through 25)
D2 - Diesel Generator 2 Supplies AC Power to Bus 1D	5.44-2	1.59-4	Page A-84 (numbers 23 through 25)

NOTE: Exponential notation is indicated in abbreviated form; i.e., 3.79-4 = 3.79×10^{-4}.

TABLE 5-6. TORNADO MISSILE SCENARIO 2 CONDITIONAL ELECTRIC POWER STATE FREQUENCIES

Electric Power State	Initiating Event Category
	Loss of Offsite Power (T4) Due to Tornado Missile
EP-1 (2 AC-Offsite, 2 DC)	0.00
EP-2 (2 AC-Diesel Generators, 2 DC)	8.93-1
EP-3 (1 AC-Offsite, 1 DC)	0.00
EP-4 (1 AC-Diesel Generator, 1 DC)	1.04-1
EP-5A (No AC, 2 DC)	2.96-3
EP-5B (No AC, No DC)	4.14-5

NOTE: Exponential notation is indicated in abbreviated form; i.e., 8.93-1 = 8.93×10^{-1}.

TABLE 5-7. LOSS OF OFFSITE POWER (T4) DUE TO TORNADO MISSILE SCENARIO 2
EVENT TREE INPUT DATA

Event Tree Top Event Description	Electric Power States Conditional Frequency of Failure (mean)						Data Source (Reference 2 if Section Number, Reference 3 if Page Number)
	EP-1 2 AC (offsite) 2 DC 0.0	EP-2 2 AC (DG's) 2 DC 8.93-1	EP-3 1 AC (offsite) 1 DC 0.0	EP-4 1 AC (DG) 1 DC 1.04-1	EP-5A No AC 2 DC 2.96-3	EP-5B No AC No DC 4.14-5	
T4 - Loss of offsite Power (6.0-6)	0.0	5.36-6	0.0	6.24-7	1.78-8	2.48-10	Product of IE and EP Frequency
RS - Reactor Scram	5.40-5	5.40-5	5.40-5	5.40-5	5.40-5	5.40-5	Page A-102
IV - MSIVs Close	5.28-4	5.28-4	5.28-4	5.28-4	5.28-4	5.28-4	Section B.5
BV - Turbine Control System Closes Bypass Valves	1.0	1.0	1.0	1.0	1.0	1.0	Assumed Failed Due to Tornado Missile
PR - Pressure Relief, EMRVs or Safety Valves Open	$< 10^{-9}$	$< 10^{-9}$	$< 10^{-9}$	$< 10^{-9}$	$< 10^{-9}$	$< 10^{-9}$	Section B.9
CV - EMRVs or Safety Valves Close	1.79-2	1.79-2	1.79-2	1.79-2	1.79-2	5.50-5	Section B.9
IC - Isolation Condenser Actuation	1.19-5	8.36-6	3.45-3	2.90-3	8.36-6	5.00-2	Section B.7

NOTES:

1. Exponential notation is indicated in abbreviated form; i.e., 8.93-1 = 8.93×10^{-1}.
2. EP = electric power; DG = diesel generator; IE = initiating event.

TABLE 5-7 (continued)

Event Tree Top Event Description	Electric Power States Conditional Frequency of Failure (mean)						Data Source (Reference 2 if Section Number, Reference 3 if Page Number)
	EP-1 2 AC (offsite) 2 DC 0.0	EP-2 2 AC (DG's) 2 DC 8.93-1	EP-3 1 AC (offsite) 1 DC 0.0	EP-4 1 AC (DG) 1 DC 1.04-1	EP-5A No AC 2 DC 2.96-3	EP-5B No AC No DC 4.14-5	
MU - Isolation Condenser Shell Side Makeup	3.96-3	3.96-3	3.96-3	3.96-3	6.48-4	6.48-4	Page A-513
CR - Control Rod Drive Flow	1.0	1.0	1.0	1.0	1.0	1.0	Assumed Failed Due to Tornado Missile
VO - EMRVs or Safety Valves Open	1.0	1.0	1.0	1.0	1.0	1.0	Assumed Failed Due to Tornado Missile
AD - ADS Actuation	1.0	1.0	1.0	1.0	1.0	1.0	Assumed Failed Due to Tornado Missile
CS - Core Spray Injection	1.0	1.0	1.0	1.0	1.0	1.0	Assumed Failed Due to Tornado Missile
CC - Suppression Pool (containment) Cooling	1.0	1.0	1.0	1.0	1.0	1.0	Assumed Failed Due to Tornado Missile

NOTES:

1. Exponential notation is indicated in abbreviated form; i.e., 8.93-1 = 8.93×10^{-1}.
2. EP = electric power; DG = diesel generator; IE = initiating event.

TABLE 5-7 (continued)

Event Tree Top Event Description	Electric Power States Conditional Frequency of Failure (mean)						Data Source (Reference 2 if Section Number, Reference 3 if Page Number)
	EP-1 2 AC (offsite) 2 DC 0.0	EP-2 2 AC (DG's) 2 DC 8.93-1	EP-3 1 AC (offsite) 1 DC 0.0	EP-4 1 AC (DG) 1 DC 1.04-1	EP-5A No AC 2 DC 2.96-3	EP-5B No AC No DC 4.14-5	
CF - CRD Flow	1.0	1.0	1.0	1.0	1.0	1.0	Assumed Failed Due to Tornado Missile
FP - Fire Protection Water to Core Spray	1.0	1.0	1.0	1.0	1.0	1.0	Assumed Failed Due to Tornado Missile

NOTES:

1. Exponential notation is indicated in abbreviated form; i.e., 8.93-1 = 8.93×10^{-1}.
2. EP = electric power; DG = diesel generator; IE = initiating event.

TABLE 5-8. SUMMARY OF RESULTS EVENT TREE T4 (TORNADO MISSILE SCENARIO 2) QUANTIFICATION

Event Sequence State			Mean Frequency (events per reactor year)	Core Melt Frequency (events per reactor year)
Success State	Transfer States			
	To Another Event Tree	To Containment Event Tree		
S1			5.87-6	
S2			0.00	
S2/F			0.00	
S3			0.00	
S3/B			0.00	
S4/F			0.00	N/A
S4/FB			0.00	
S5/F			0.00	
S5/FB			0.00	
S6			0.00	
S6/B			0.00	
	L1		6.00-15	
		ELDF	1.07-7	
		ELDS	0.00	
		EHD-	2.51-8	1.4-7
		ELDFB	0.00	
		ELDSB	0.00	
		EHD-B	3.17-9	
		ATWS	3.23-10	

NOTE: Exponential notation is indicated in abbreviated form; i.e., 5.87-6 = 5.87×10^{-6}.

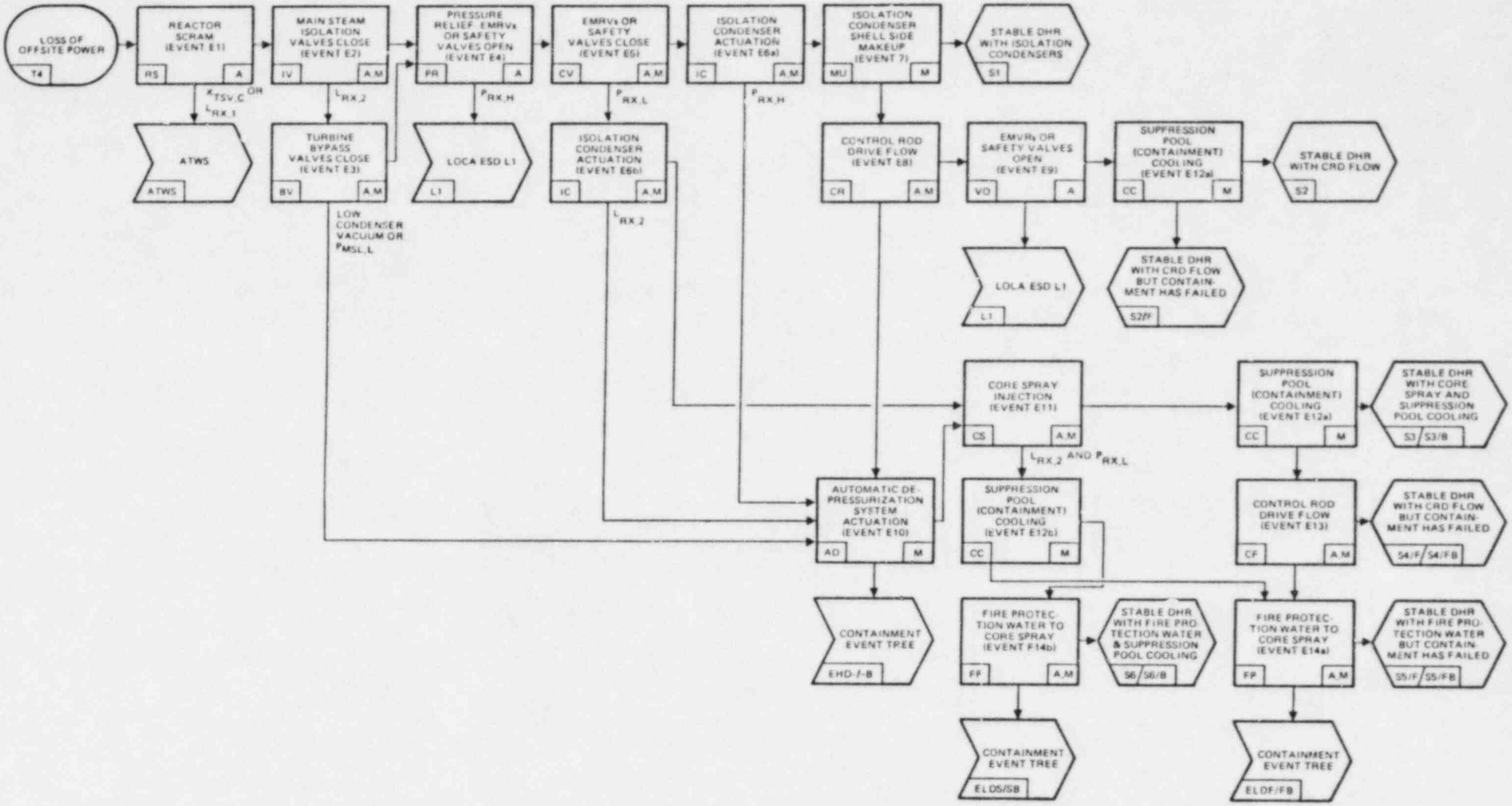

FIGURE 5-1. LOSS OF OFFSITE POWER EVENT SEQUENCE DIAGRAM T4

RELEASE CATEGORY EVENT TREE PLOT DATE 82/12/29.

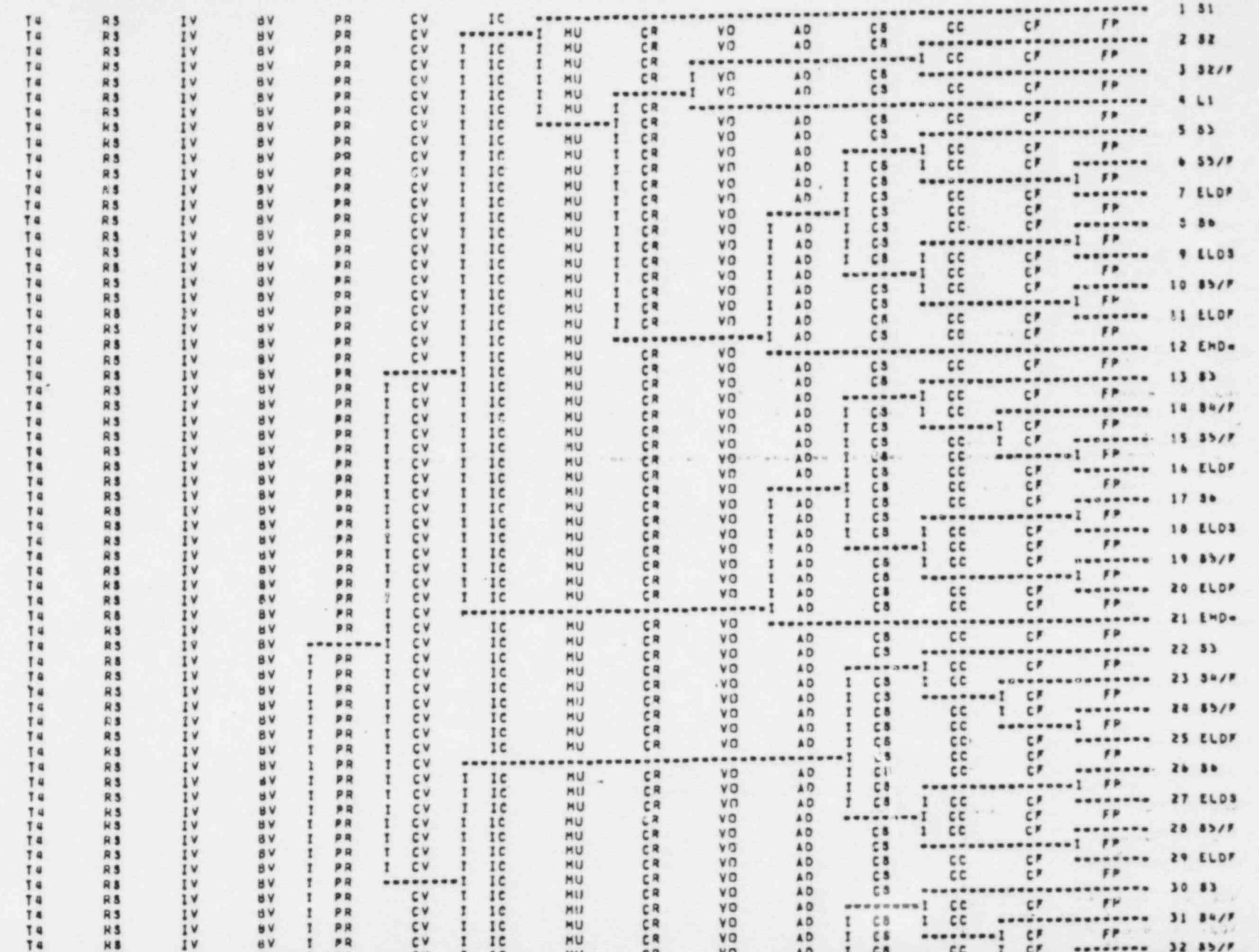

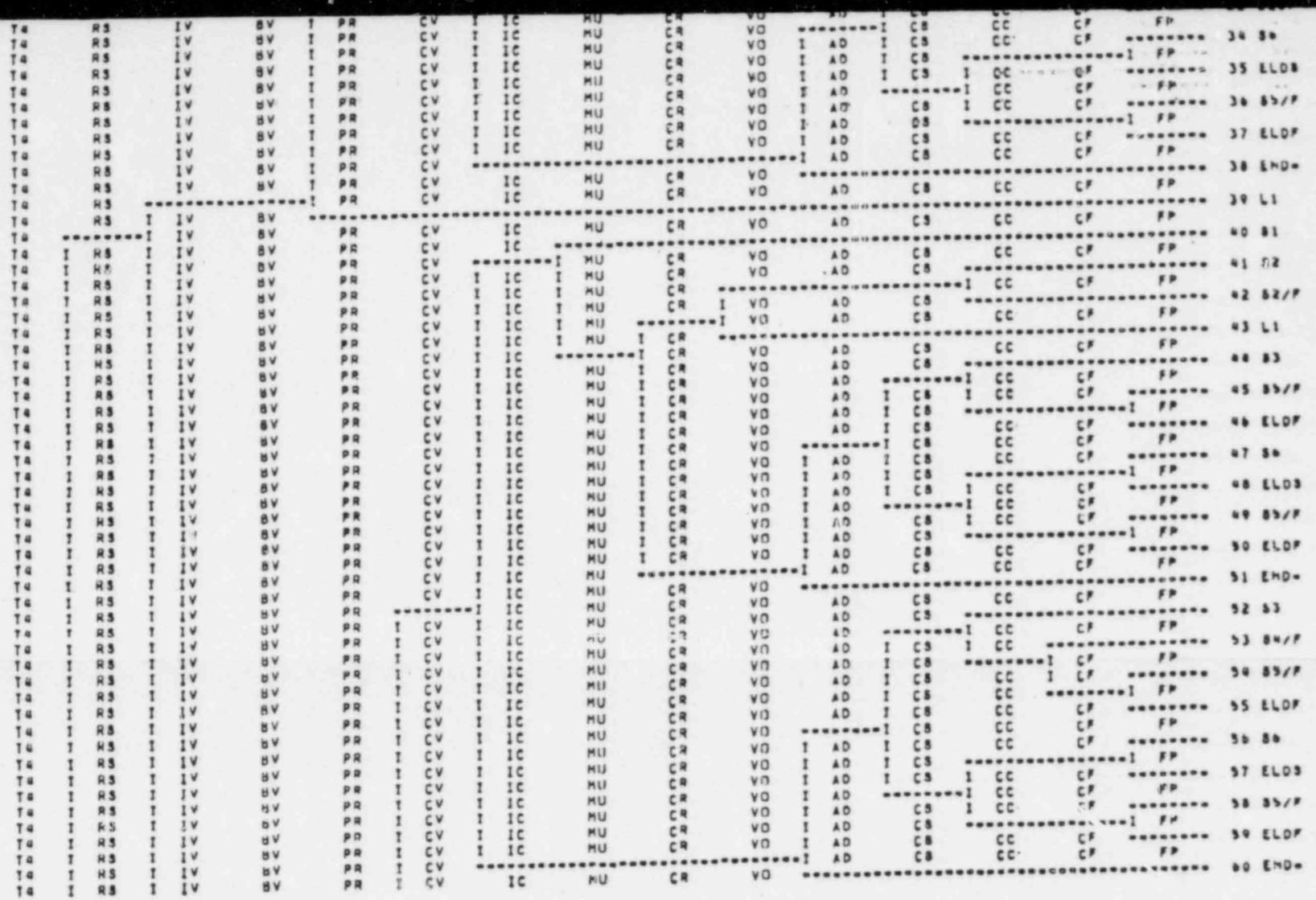

FIGURE 5-2. LOSS OF OFFSITE POWER EVENT TREE T4
(Sheet 1 of 2)

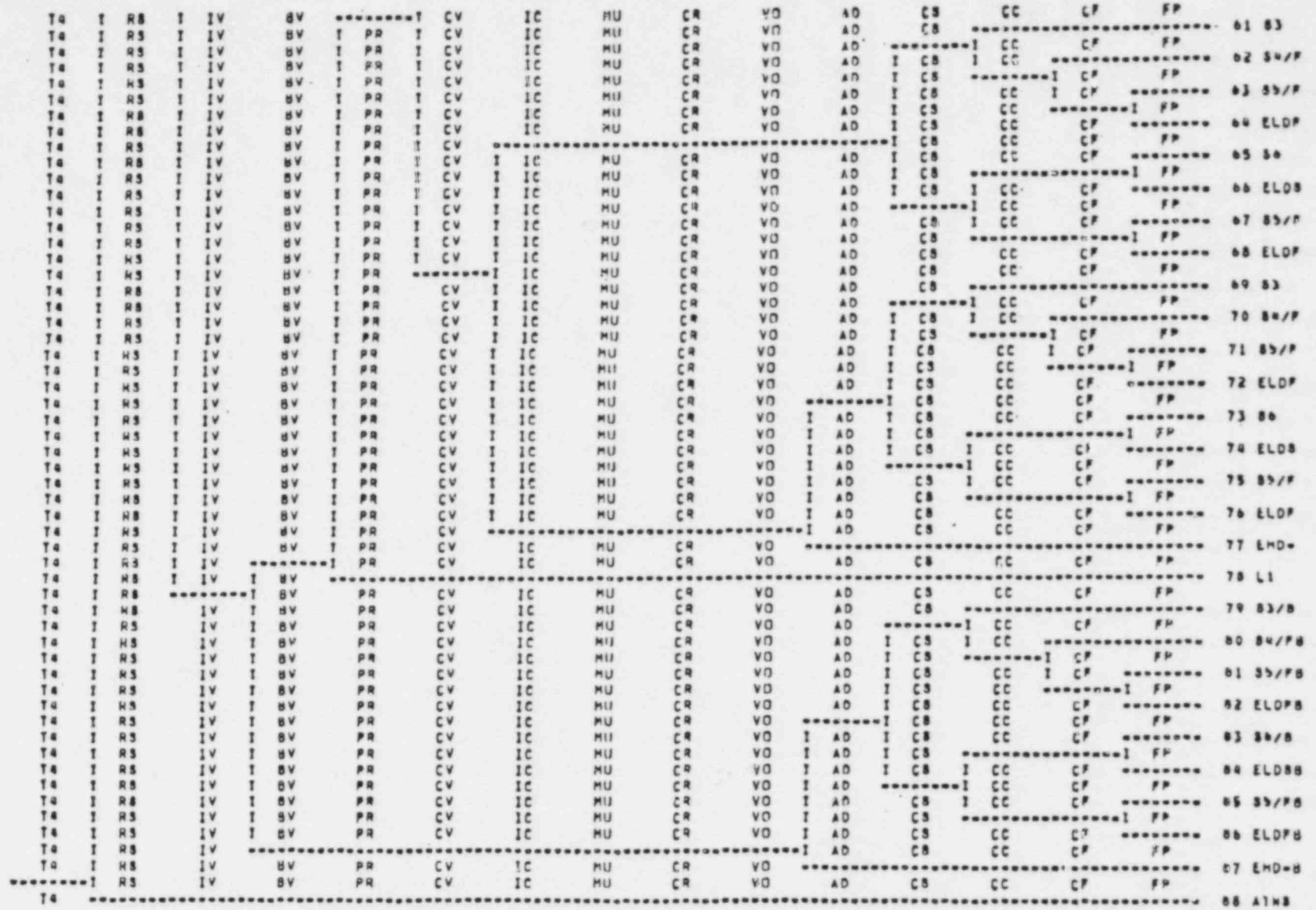

FIGURE 5-2 (continued)
(Sheet 2 of 2)

6. REFERENCES

1. Twisdale, Lawrence A., and William L. Dunn, "Tornado Windspeed and Missile Risk Analysis of Cable Tray Bridges at Oyster Creek Nuclear Generating Station," Research Triangle Report 44T-2382, April 1982.

2. Garrick, B. John, et al, "Oyster Creek Probabilistic Safety Analysis, Plant Analysis Update," PLG-0253, December 1982.

3. Garrick, B. John, et al, "OPSA, Oyster Creek Probabilistic Safety Analysis," Executive Summary, Main Report, and Appendices, Draft Report, PLG-0100, August 1979.

APPENDIX

TORNADO WINDSPEED AND MISSILE RISK ANALYSIS OF CABLE TRAY BRIDGES AT OYSTER CREEK NUCLEAR GENERATING STATION

JCP&L-DOC-03

RESEARCH TRIANGLE INSTITUTE

April 1982

Final Report 4AT-2382

TORNADO WINDSPEED AND MISSILE RISK ANALYSIS OF CABLE TRAY BRIDGES AT OYSTER CREEK NUCLEAR GENERATING STATION

Prepared for

Pickard, Lowe and Garrick
17840 Skypark Boulevard
Irvine, California 92714

Under

Purchase Order N3 1033

Prepared By

L. A. Twisdale
W. L. Dunn

TABLE OF CONTENTS

I. INTRODUCTION

The objective of this investigation was to estimate tornado windspeed and missile loading probabilites for parallel cable tray bridges at the Oyster Creek Nuclear Generating Station. Information on the site location and the bridge structures were provided by Pickard, Lowe and Garrick, Inc.

The scope of this investigation has consisted of:

1. Computer simulations of tornado strike on the plant to develop a function of the annual probability tornado windspeed exceedance. Previously developed regional tornado data from the 1950-1978 National Severe Storms Forecast Center (NSSFC) was used for these calculations with a 360 mph upperbound intensity given by the NRC Region I design basis tornado.
2. Computer simulations of tornado generated missiles to develop functions of annual probability of impact and plate perforation versus bridge plate thickness. Probabilities of damaging the parallel bridge structures in the same tornado event have also been estimated.

The methodology and tornado data base follow the models and analyses described in Refs. 1-9. The tornado windspeed calculations were made using the TORRISK simulation code that takes into account structure size, geometry, and height above grade. Based on 1000 tornado strike simulations of each F-scale intensity category, the fastest quarter mile windspeed corresponding to a 10^{-7} annual exceedance probability was estimated as 300 mph for these two structures. The TORMIS simulation computer code was used to estimate the tornado missile impact and bridge plate perforation probabilities. The

results of over 32,000 individual missile simulation histories indicate that the probability of tornado missiles perforating both bridge structures is less than 10^{-7} per year for 0.25 inch plate thickness. This report documents the input data used in the investigation and summarizes the methodology and results.

II. METHODOLOGY

A. Introduction

A methodology for assessing the probabilities of tornado and tornado missile related events has been developed for nuclear plant risk analysis and is documented in Refs. 1-9. These models and the tornado data base have been integrated to form a Monte Carlo simulation methodology for predicting tornado windloads and missile effects on structures. The relevant elements of this methodology are applied herein to assess the tornado windspeed and missile loading risk for cable tray bridge structures at the Oyster Creek Nuclear Generating Station. In the following paragraphs of this section, a brief review is presented of the tornado windspeed and tornado missile loading prediction methodology.

B. Tornado Windspeed Risk Model

The tornado wind-risk calculations are based on a Monte Carlo procedure that uses a stochastic model of tornado occurrence, a probabilistic tornado windfield model, and distributions of tronado parameters developed from an analysis of 19,085 storms.

1. Tornado Risk Model

Assuming that the occurrence of tornado events constitutes a Poisson process with mean occurrence rate ν, the probability that the windspeed v exceeds a maximum horizontal velocity V^*, $P(v > V^*)$, during time T is given by

$$P_T(v > V^*) = 1 - \exp\left[-\nu\, P(v > V^*)T\right] \qquad (1)$$

as derived by Wen and Chu [10]. For $\nu\, P(v > V^*)T < 0.01$, Eq. 1 can be approximated by

$$P_T(v > V^*) \cong \nu\, P(v > V^*)T \qquad (2)$$

with an accuracy of 0.5 percent. Hence Eq. 2 is valid for rare events such as tornado strike. The robustness of Eq. 1 when compared to a more general tornado arrival process has been indicated in Ref. 5. In addition, Twisdale et al. [8] develop analogous expressions for the Weibull, Bayesian-Poisson, and Bayesian-Weibull processes and conclude that Eq. 2 is an accurate approximation when compared to other arrival processes with comparable values of ν.

Consistent with the discrete nature of the tornado FPP (Fujita intensity, Pearson path length, Pearson path width) classification system [e.g., 11], $P(v > V^*)$ is evaluated from the total probability equation

$$P(v > V^*) = \sum_{i=0}^{F_{max}} P(v > V^* | F_i)\, P(F_i) \qquad (3)$$

where F_i denotes the F-scale classification and F_{max} the upperbound tornado intensity.

2. Tornado-Target Strike Model

The tornado strike model developed in Ref. 1 for nuclear power plant risk assessment includes the plant geometry in the risk calculation. By modeling the tornado damage path as a rectangle with length L_t and width W_t, an expression for the tornado strike probability was developed that is valid for any nonreentrant polygon enclosing the plant safety-related systems. In the Monte Carlo analysis, an estimate of the windspeed exceedance probability event $P(v > V^*)$ for the jth simulation of tornadoes with intensity F_i is given by

$$P_j(v > V^* | F_i) = \frac{(A_o)_j}{S} \quad , \tag{4}$$

where $(A_o)_j$ is the tornado origin area within which $v > V^*$ and is given by

$$(A_o)_j = (W_t^*)_j (L_t^*)_j + (W_t^*)_j (Z_l)_j + (L_t^*)_j (Z_w)_j + A_T \tag{5}$$

and S is the tornado reference area used in the assessment of the tornado occurrence rate, ν. In Eq. 5, $(W_t^*)_j$ and $(L_t^*)_j$ are the values of W_t and L_t, respectively, for the j^{th} tornado within which $v > V^*$; $(Z_l)_j$ = maximum projection of target polygon in the tornado length direction; $(Z_w)_j$ = maximum projection of target polygon in tornado width direction; and A_T = area of the target. Z_l and Z_w depend upon the target geometry and tornado direction, ϕ_t. The calculation represented by Eq. 4 is based on the assumption that tornado occurrence is uniformly random over the reference area S. The calculation of A_o in Eq. 5 corresponds to a union definition of tornado-target interaction in which windspeed exceedance is defined if any portion of the target experiences windspeeds greater than V^*. This definition of tornado strike is thus appropriate for the cable tray bridge design calculations of tornado windspeed risk.

3. Tornado Windfield Model

The synthesized tornado windfield model originally developed for the probabilistic assessment of tornado hazard risk is documented in Refs. 1, 3, 7 and 8. In Ref. 8, sensitivity analyses and pairwise comparisons of the model to the Fujita DBT-77 [12], the Fujita suction vortex DBT-78 [12], and the TRW Phase III models [13] are given. The model is shown to be robust for tornado missile predictions with the most important parameters being the translational

speed (U_T), the ratio of radial to tangential components magnitudes (γ), and the radius to the maximum windspeed (R). In Ref. 8, the windspeeds are shown to be much less sensitive to the core slope (S) and boundary layer thickness (δ_o) parameters. The probabilistic characterization of these variables was updated to reflect the best estimates of tornado vortex flow parameters.

For the windspeed exceedance probability calculations, the synthesized windfield model is used to define the vertical and lateral windspeed variation in the windfield. This is accomplished by sampling from the distributions of U_T, γ, R, S and δ_o for the sampled maximum windspeed, $(U_{max})_j$, and $(W_t)_j$ path width. Then additional parameters are calculated to match the windfield boundary [cf. 3,8]. The determination of $(W_t^*)_j$, within which $v > V^*$, is determined from an analytic solution of the resultant horizontal wind velocity expression as a function of offset from the vortex center, as illustrated in Fig. III-1.

4. Path Length Intensity Variations

In addition to the variation in maximum tornado windspeed experienced across the path width, tornado intensity varies along the path length. This variation is well documented in terms of both observed damage characteristics and photographs of the life cycle features of several tornadoes. Damage assessment mapping provides a data base for the determination of $(L_t^*)_j$ within which $v > V^*$ for the windspeed exceedance probability calculation. The analysis in Ref. 8 includes 150 observations from the April 3-4, 1974 tornado outbreak [14], the Red River Valley tornado outbreak of April 10, 1979 [15], the Bossier City, Louisiana tornadoes [16], the Grand Gulf, Mississippi tornadoes [17], and the Cabot, Arkansas tornado [18].

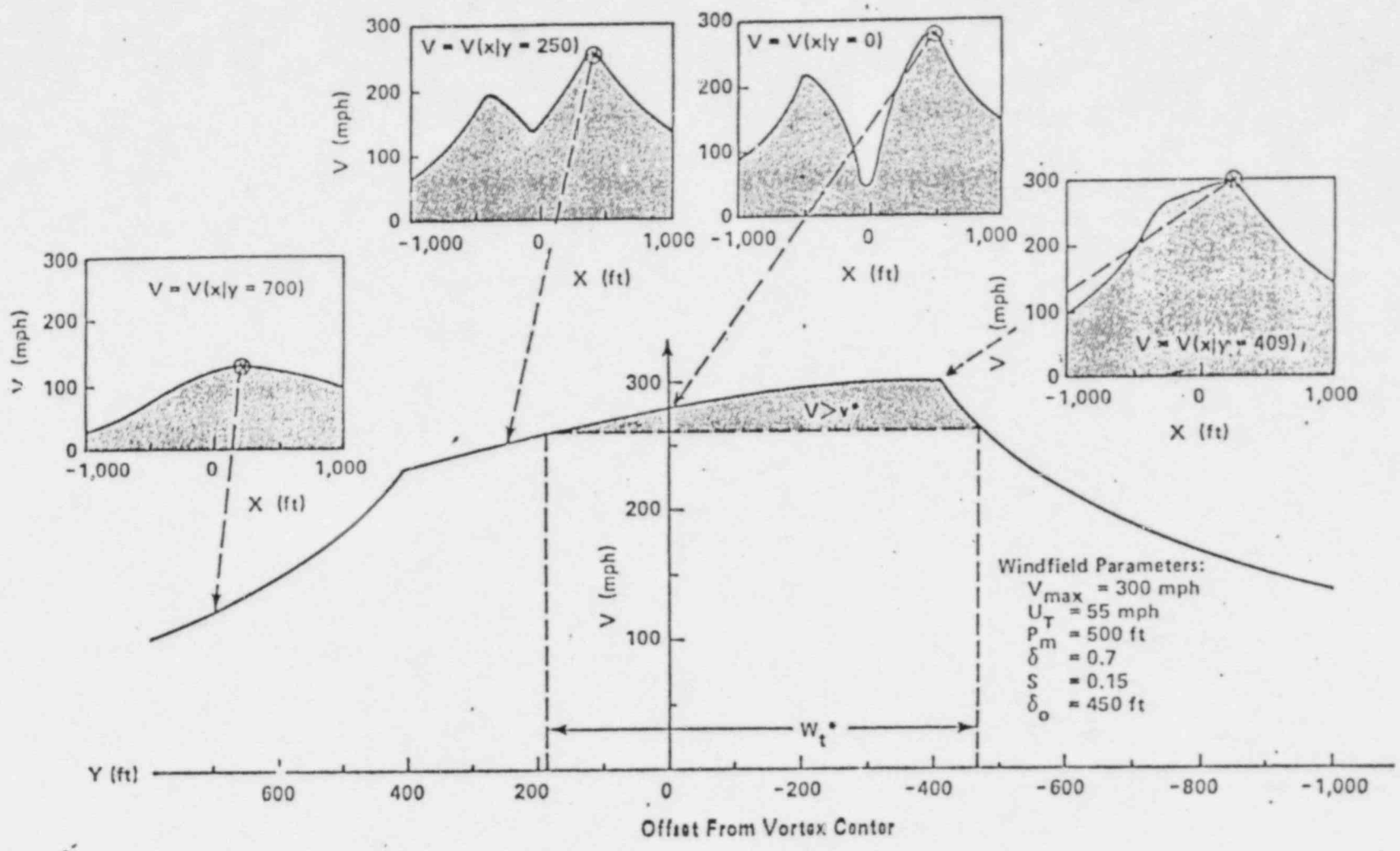

Figure II-1. Loci of peak horizontal windspeeds

5. Probabilistic Model of Tornado Data

The prediction of the probability that a tornado with maximum windspeed U_{max} will strike a nuclear power plant requires information on tornado incidence, e.g., ν in Eq. 1; tornado intensity distribution, $P(F_i)$ in Eq. 3; and the tornado path characteristics (e.g, W_t^*, L_t^*, and ϕ_t as implied in Eq. 5). This information is specified by the mean occurrence rate ν, a joint probability density function $f_{F,P_L,P_W,\Phi_t}(F,P_L,P_W,\Phi_t)$, and the relationships between P_L and L_t, between P_W and W_t, and between Φ_t and ϕ_t. In this notation, F, P_L, and P_W are the classification integers in the FPP tornado classification system and Φ_t is the octant (N,NE,E,...,NW) defining the tornado path direction. Based upon the hypothesis tests in Refs. 1 and 4, the following representation of the above density function is adopted.

$$f_{F,P_L,P_W,\Phi_t}(F,P_L,P_W,\Phi_t) = f_F(F) \cdot f_{P_L|F}(P_L|F) \cdot$$

$$f_{P_W|P_W,F}(P_W|P_L,F) \cdot f_{\Phi_t}(\Phi_t) \qquad (6)$$

For the j^{th} simulation of tornado intensity F_i in the Monte Carlo analysis, the multivariate set $\{F,P_L,P_W,\Phi_t\}$ is obtained by sampling in sequential order from the discrete functions represented by Eq. 6. Then the continuous variables are obtained by sampling

$$f_{U_{max}|F_i}(U_{max}|F_i) \rightarrow (U_{max})_j \qquad (7a)$$

$$f_{L_t|P_{L_i}}(L_t|P_{L_i}) \rightarrow (L_t)_j \qquad (7b)$$

$$f_{W_t|P_W}(W_t|P_W) \rightarrow (W_t)_j \tag{7c}$$

$$f_{\phi_t|\phi_t}(\phi_t|\phi_t) \rightarrow (\phi_t)_j \tag{7d}$$

to obtain $(U_{max})_j$, $(L_t)_j$, $(W_t)_j$, and $(\phi_t)_j$. The variables are then employed in the Monte Carlo calculations as noted in the following subsection.

6. Simulation Methodology

Probabilistic Monte Carlo techniques are used to estimate the tornadic windspeed exceedance probabilities. The TORRISK simulation code has been developed to produce numerical estimates of $P(v > V^*)$. First, the tornado characteristics are sampled, then the path area within which $v > V^*$ are determined and the tornado origin areas are calculated for a series of windspeed intensity levels. By stepping through a series of V* for each tornado, matrices of $E[(A_o)_{ki}]$ and $\sigma^2[(A_o)_{ki}]$ are determined by simulating a large number of tornadoes from each intensity category. The annual windspeed exceedance probabilities are estimated from

$$\hat{P}(v > V^*) = \nu \sum_{k=i}^{F_{max}} P(F_k)E(A_o)_{ki} \tag{8}$$

where ν is expressed in tornadoes/sq mi/yr. The statistical confidence bounds are determined in the conventional manner with

$$P\left[\hat{P}(v > V^*) - T_{\alpha/2}\frac{\hat{\sigma}[P(v>V^*)]}{N} < P(v > V^*) < \hat{P}(v > V^*) + T_{\alpha/2}\frac{\hat{\sigma}[P(v > V^*)]}{N}\right] = 1 - \alpha \tag{9}$$

where $T_{\alpha/2}$ is the value of the standard normal variate with cumulative probability level $1 - \alpha/2$ and

$$\hat{\sigma}^2 [P(v > V^*)] = v^2 \sum_{k=i}^{F_{max}} P(F_k)^2 \sigma^2[(A_o)_{ki}] \quad . \tag{10}$$

C. Tornado Missile Risk Model

A sequence of events must occur for a safety-related component at a nuclear plant to be impacted and actually damaged by a tornado-generated missile. First of all, a tornado must occur and pass through the plant site area. As noted previously, the national tornado data record has been analyzed to provide input information to the risk analysis on tornado occurrence rates and strike characteristics. The investigation included analyses of the potential for tornado classification error based upon storm damage interpretations and the lack of a damage medium (structures, vehicles, trees, etc.) in some regions. The research also addressed the uncertainty in windspeed ranges and the variation of storm intensity along the path length. Combination of these analyses resulted in a methodology to assess tornado strike probabilities and quantified input for tornado regions in the United States.

A tornado windfield model was also developed to be compatible with the entire range of observed windfield intensities and path widths. Tornado flow characteristics were identified that were potentially significant in terms of missile transport phenomena. In order to account for both modeling uncertainty and the natural variability observed among tornadoes, several random variables were specified in the model, including tornado intensity, path width, translational speed, radius to maximum tangential velocity, ratio

of the radial to tangential wind speeds, vertical variation of core size, and boundary layer thickness. In view of the difficulty in establishing a priori conservative flow characteristics for missile transport, the windfield model was synthesized from theoretical, observational, and probabilistic considerations. A significant aspect of the model is that the parameters can be adjusted to make the intensity, size, and velocity variables consistent with the tornado path width boundary specifications.

Another component in the hazard must be the availability of objects in the plant vicinity before any missiles can be generated. These objects must be accelerated by the tornado winds to pose a potential threat to any of the plant's safety systems. A missile transport model was needed that would be efficient to permit simulation studies of thousands of trajectories and yet describe the expected variance of turbulent tornado transport. A random orientation transport model was developed and statistically verified through a series of comparisons to both simplified three-degree-of-freedom and rigid body six-degree-of-freedom trajectory models. The missile injection methodology was developed to provide for missile release to the moving tornado when the restraint forces are exceeded by the tornado-induced aerodynamic forces. A simulation study was performed to determine the optimum specification of missile restraint forces to ensure conservatism in this component of the mechanistic analysis.

Finally, if the potential missile is transported by the tornado, it must hit a "target" or safety related system to pose an actual threat to the operation of the plant. An impact methodology was developed for a spectrum of missiles to provide a basis for predicting structual damage, given an impact. Recent impact test data were used in a probabilistic approach to account for

structural strength variations and random impact orientations. An analytical study of oblique missile impact was also performed [1,6,8]. For metal missiles impacting steel plate targets, the BRL formula [19] is used to assess perforation damage. For wood missiles impacting steel plate targets, the perforation equation developed by Baker et al. [20] is used. Appendix A summarizes these expressions.

These components of the tornado missile hazard were linked together to form an integrated model of the process as indicated in Fig. II-2. Approximately 25 random variables were used to characterize the modeling uncertainty, natural variability of tornado events, and the site-specific characteristics at a particular plant. The risk assessment methodology is based upon the specification of the probability models for these variables, identification of the output sample space, and the use of simulation techniques to assign probabilities to this sample space.

1. The Probabilistic Simulation Model

The probability model that is adopted to simulate tornado missile events is based on the following hypothesis:

(1) A finite and deterministic number (N) of potential missiles exists in the plant vicinity over a specified time interval; these objects are assumed to define the risk-contributing missile population.

(2) Within the sampling population N, or a subpopulation of it, each potential missile has an equally likely chance to be transported by each tornado that strikes the plant.

(3) Multiple missile events occur sequentially and independently.

(4) The outcomes for target impact form a discrete event space.

(5) Individual missile events, including ground interaction and missile termination, do not affect the governing sampling distributions of the process.

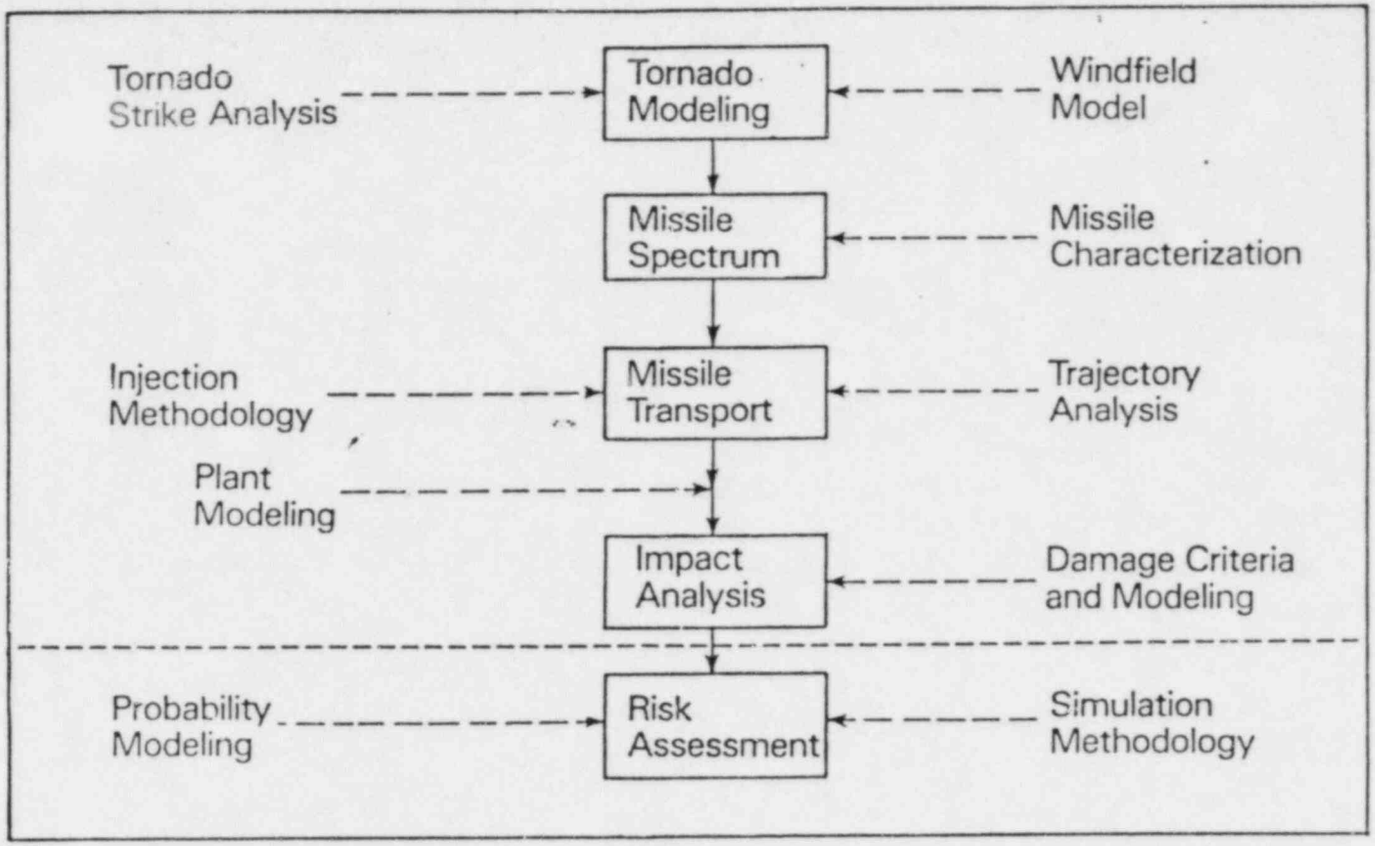

Figure II-2. Probabilistic Analysis of the Tornado Missile Hazard

These hypotheses form a basis for interpreting the resulting probability estimates from the simulations. The deterministic restriction on N in the first hypothesis results in considerable simplification in the event space specification, as well as in the probability estimation, and can be easily managed through conservative specification. Thus, dynamic modeling of N over multiple time intervals requires separate analyses that can be combined to yield the appropriate risk. The second hypothesis ensures that a random sampling scheme, using the common missile input distributions, is applicable. The assumption of mutual independence in the third hypothesis means that the response and outcome of the jth missile does not influence the response and outcome for the i^{th} missile. It thus implies an approximation to the true stochastic nature of the problem through the use of a sequential model of multiple missile events rather than a "simultaneous" model with time history superpositions. This sequential structure eliminates the specific consideration of actual missile-missile collision events in the sampling experiment. Although such events can be easily visualized as occurring in an actual tornado strike, their explicit modeling is considered to be a second-order effect. Furthermore, the probabilistic missile injection and transport methodology indirectly recognizes such sources of randomness. Hypothesis 4 above, is simply a statement of the discrete nature of missile impact events; i.e., a missile cannot partially impact a target. The final hypothesis specifies that a missile history does not affect the sampling distributions for subsequent histories in the same tornado event. Statistically, this suggests independence among the missile histories in the sense that the sampling distributions remain unchanged for a given tornado event.

2. Single and Multiple Missile Events

The analysis of impact and damage probabilities for tornado generated missiles under typical nuclear power plant operating conditions requires an assessment for a spectrum of potential missiles. The types and numbers of these objects are assumed to define a population of N potential missiles. The objective of the risk analysis is to predict the effects on the plant of the postulated population of the N objects. Since, in general, there is no physical mechanism that restricts the number of missiles that may be generated during a tornado strike to one, multiple missile risk probabilities are implied in the risk assessment. Hence, the probabilistic formulation must account for the fact that from 0 to N missiles may be generated during a tornado strike.

A multiple missile and multiple target probability event space was developed in Ref. 1 for tornado missile hazard assessment. By treating the missiles as indistinguishable (nonordered) points in the sample space, and by assuming mutual independence,[1] the following relationship was developed for a single target A_h:

$$P^N(A_h|I_\ell)_j = 1 - [1 - P(A_h|I_\ell)_j]^N \quad , \tag{11}$$

where the notation $P(A_h|I_\ell)_j$ is the single missile probability that event A_h occurs during the jth tornado strike of tornadoes with intensity characteristic I_ℓ and $P^N(A_h|I_\ell)_j$ is the multiple missile probability. This simple model (referred to as the Bernoulli model) was shown to give accurate

---

[1] The assumption of mutual independence means that the missile trials are repeated under identical conditions for the assumed tornado and that the jth trial does not influence the outcome of the ith trial for $j \neq i$.

predictions as compared to a model based on individually ordered missiles, the so-called Poisson trials model [cf. 21]. The following fundamental inequality was derived:

$$E\{1-[1 - P(A_h|I_\ell)_j]^N\} \leq 1-[1- P(A_h|I_\ell)_j]^N \leq 1 - \prod_{i=1}^{N} [1 - P(A_h|I_\ell,M_i)_j] \quad , \tag{12}$$

where $P(A_h|I_\ell,M_i)_j$ is the probability of event A_h due to missile M_i. In Eq. 12, the Poisson trials model is the right-hand or upperbound probability. For small $P(A_h|I_\ell)_j$, the Bernoulli model was shown to be within a few percent of the "finer grained" Poisson trials model and hence to be an accurate predictor for tornado missile events. The lower-bound inequality in Eq. 12 means that the expectation of the Bernoulli model, with $P(A_h|I_\ell)_j$ being considered as a random variable, yields a lower multiple missile probability than that predicted with the mean value of $P(A_h|I_\ell)_j$.

Multiple target events include union and intersection event combinations of single targets. For q targets A_1, A_2,...A_q, the probability that at least one is damaged during tornado strike $(I_\ell)_j$ is

$$p^N[(A_1|I_\ell)j \quad (A_2|I_\ell)_j \quad . \; . \; . \quad (A_q|I_\ell)_j] = 1 - [1 - \sum_{i=1}^{q} P(A_i|I_\ell)_j]^N \quad , \tag{13}$$

as developed in Ref. 1 for a union event combination of two targets. The probability that all q targets are damaged (the intersection event) during the tornado strike is given by

$$P^N[(A_1|I_\ell)_j \quad (A_2|I_\ell)_j \quad . \; . \; . \quad (A|I_\ell)_j] = 1 - \sum_{i=1}^{q} [1 - P(A_i|I_\ell)_j]^N +$$

$$+ \sum_{k>i} [1 - P(A_i|I\ell)_j - P(A|I_\ell)_j]^N -$$

$$- \sum_{m>k>i} [1 - P(A_i|I_\ell)_j - P(A|I_\ell)_j - P(A_m|I_\ell)_j]^N + \; . \; . \; . \; . \qquad (14)$$

Eqs. 13 and 14 provide the basis for assessing damage probabilities for various target combinations. For example, multiple missile damage probabilities that both cable tray bridges are damaged in the same tornado event is given by Eq. 14 with q = 2. In Ref. 8, these expressions are generalized to include a subpopulation approach in the specification of N.

3. Simulation Methodology

Probabilistic Monte Carlo simulation [e.g., 22,23] is used to estimate the missile event probabilities--e.g., $P(A|I_j)$--because of the complex and multidimensional form of the random process. The TORMIS simulation code has been developed to produce numerical estimators of both single and multiple missile event probabilities. The output consists of statistically independent outcomes, each of which follows the same probability law. The expected value and variance are the population descriptors evaluated explicitly in the TORMIS code. For a mathematical statement of the tornado missile simulation, it is convenient to introduce the functions $g(\bar{x}|\bar{z})$ and $h(\bar{z})$ to represent the complete stochastic process. The random process for the tornado definition and occurrence is defined by $h(\bar{z})$, where $\bar{z}$ is a vector of tornado random variables. The function $g(\bar{x}|\bar{z})$ denotes the tornado missile random process in which $\bar{x}$ is a vector of missile random variables. Thus, the complete stochastic process is given by the product $g(\bar{x}|\bar{z})h(\bar{z})$; the notation

for an outcome is $g(\bar{X}_i|\bar{Z}_j)h(\bar{Z}_j)$, where $\bar{X}_i$ denotes the i^{th} vector of tornado variables sampled from $f(\bar{x})$. For a single missile history, the outcome relative to some defined event A is a random variable "a." This outcome being denoted as $g_A(\bar{X}_i|\bar{Z}_j)h_A(\bar{Z}_j)$, the characteristics of the probability law of "a" can be inferred from n independent observations. The expected value of "a" is estimated by

$$\hat{E}(a|I) = \frac{1}{m} \sum_{j=1}^{m} h_A(\bar{Z}_j) \frac{1}{n} \sum_{i=1}^{n} g_A(\bar{X}_i|\bar{Z}_j), \qquad (15)$$

where $n = m \cdot n$. For the Bernoulli trial model, the probability of success of A is given by this expectation, and hence $P(A) = E(a)$ and $P(A) = E(a)$. The estimate of $P(A|I_j)$ is given by the right summation in Eq. 15. It is noted that for single missile events the estimation of $P(A|I)$ is not dependent upon the division of m and n for large n, provided that a reasonable number (m) of tornadoes is considered and n is sufficiently large. However, for multiple missile events, n must be large enough to provide an estimate of $P(A|I_j)$, which can be used in the analytical expressions derived previously. Thus, the estimation accuracy of $P(A|I_j)$ is useful; the sample variance, $\sigma^2(a|I_j)$, and the variance of $P(A|I_j)$ follow the standard forms [22]. In the TORMIS code, confidence bounds are calculated assuming normality, which has been shown to give accurate results compared to a modified binomial sampling procedure [1].

III. PROBLEM DESCRIPTION AND SIMULATION INPUTS

A. Plant Definition

The cable tray bridges at Oyster Creek Nuclear Generating Station span approximately 94 feet between the reactor and turbine buildings. The bridge structures are about 11.5 ft wide and 9.5 ft high with the top of the bridge plate located 62 feet above grade elevation. The structures are separated by a horizontal distance of 4 feet. To simulate the tornado wind and missile threat to these parallel steel bridges, the adjacent structures shown in Fig. III-1 were modeled. Targets 1 and 2 specify the North and South bridge structures, respectively. For the tornado strike and windspeed simulations, the probability of severe wind loads interacting with at least one point on these two structures is estimated using the TORRISK code. For the missile simulations, seven additional structures in the proximity of these bridges were modeled. Target 3 is the main bay and Target 4 is the reheater bay of the turbine building. Target 5 is the mechanical equipment room, which is located underneath the west portion of the cable tray bridges. Target 6 is an office building located between the turbine and reactor buildings. The reactor building is Target 7; the maintenance building north of the turbine building is Target 8; and the new redwaste building is Target 9. The turbine, reactor, and new redwaste buildings were modeled in TURMIS up to elevations that would resist tornado winds. Other structures and components in the vicinity of the cable tray bridges were not explicitly modeled, but missile sources and injection heights were specified to account for failure of non-tornado proof buildings. Hence, only the major "shadows" were modeled in the

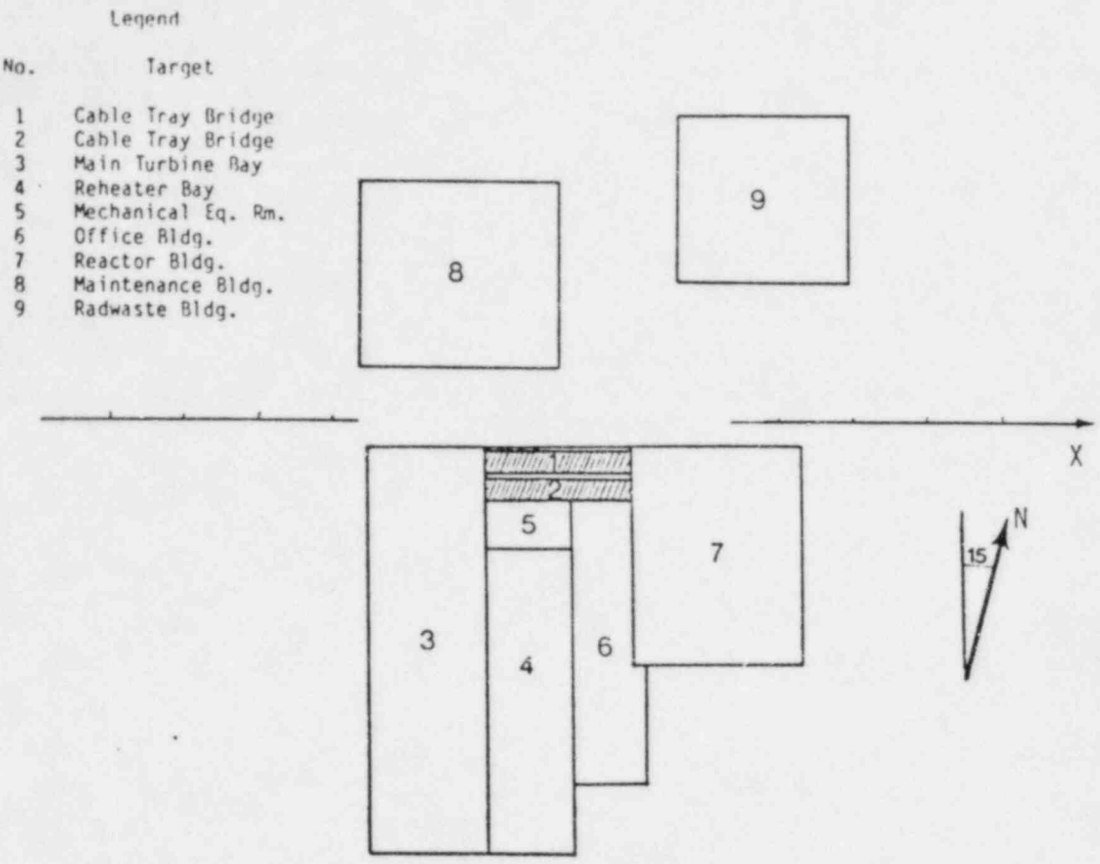

(a) Target Plan View

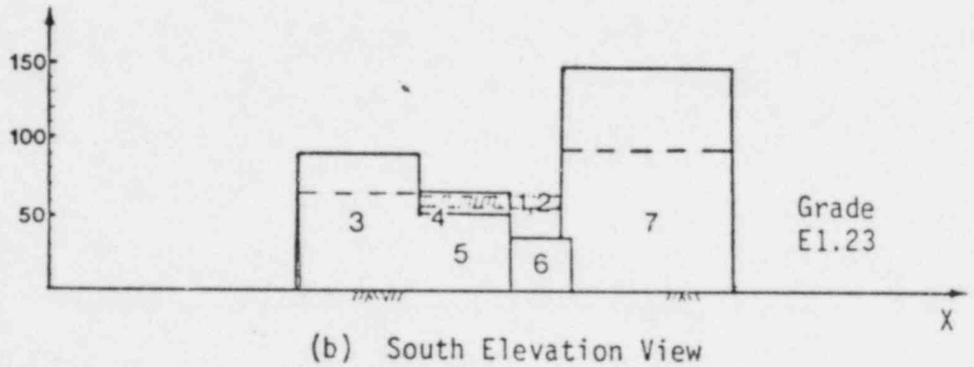

(b) South Elevation View

Figure III-1. Plan and Elevation Views of Plant Targets

missile simulations and the shadowing effects of other structures were conservatively ignored in the missile simulations.

B. Postulated Missile Threat

The missile threat that was postulated for the cable tray bridge structures included buildings, loose objects, construction materials, vehicles and other sources over the plant site area. As noted in Fig. III-2, a total of 13 areas were used to identify different missile origin zones. The zones include storage and laydown areas. parking, switchyard, and adjacent open regions. These areas include the contiguous land region within the plant protected area and extends to about 1000 ft from the bridge targets. It is noted that previous simulations of missile trajectories and field observations suggest that the greatest hazard is from potential missiles that originate within several hundred feet of the target.

The numbers of each of the standard missile types [24] postulated by zone is summarized in Table III-1. A total of 10,730 potential missiles were specified to simulate the missile sources within these contiguous zones. These missiles were specified to originate at heights that simulate the storage characteristics above grade and missiles originating due to failure of nontornado proof structural elements. The zone elevation and maximum injection heights are given in Table III-2. The minimum injection height was conservatively considered to be five feet above the zone grade elevation or the structure origin source. The missiles were uniformly injected over the interval defined by these minimum and maximum heights for each zone. The automobile was injected at a constant height of five feet above grade for all zones.

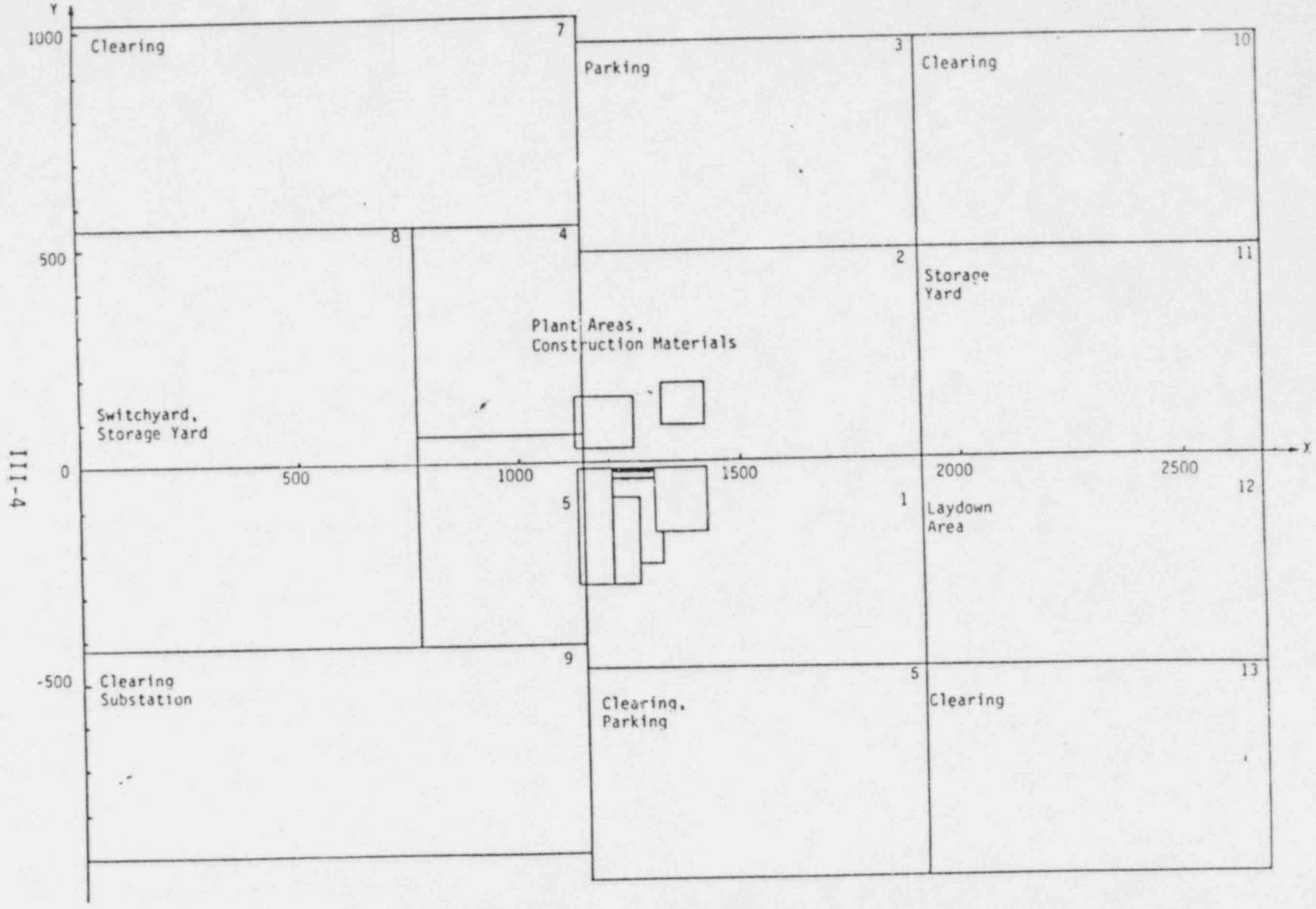

Figure III-2. Potential Missile Origin Zones

TABLE III-1. MISSILE SPECIFICATION BY ZONE

Missile Origin Zone	Number of Missiles By Type						Totals
	1-in Rod	3-in Pipe	6-in Pipe	12-in Pipe	Wood Plank	Auto	
1	200	200	200	200	200	100	1,100
2	500	500	500	500	500	50	2,550
3	100	100	100	100	100	250	750
4	100	100	100	100	100	250	750
5	100	100	100	100	100	20	520
6	100	100	50	50	250	100	650
7	10	10	10	10	10	10	60
8	200	200	200	200	200	10	1,010
9	100	100	10	10	100	10	330
10	10	10	10	10	100	10	150
11	200	200	200	200	200	10	1,010
12	200	200	200	200	200	100	1,100
13	10	10	10	10	100	10	150
14 (Str. 3)	75	50	50	25	0	0	200
15 (Str. 7)	75	50	50	25	0	0	200
16 (Str. 9)	75	50	50	25	0	0	200
Totals	2,055	1,980	1,840	1,765	2,160	930	10,730

TABLE III-2. MISSILE INJECTION HEIGHT BY ZONE

Missile Origin Zone	Injection Height Interval	Injection Height (ft) Above Grade					
		1-in Rod	3-in Pipe	6-in Pipe	12-in Pipe	Wood Plank	Auto
1,2,4,5,11,12	Min	5	5	5	5	5	5
	Max	25	25	25	25	25	10
3,6,7,10,13	Min	5	5	5	5	5	5
	Max	10	10	10	10	10	10
8,9	Min	5	5	5	5	5	5
	Max	40	40	40	40	10	10

C. Tornado Hazard

The input data for the tornado hazard definition was taken from an analysis of 19,085 tornado data entries reported in the 1950-1978 NSSFC data base [25]. Specifically, the data for tornado Region C in Ref. 8 was used in the specification of tornado intensity, path width, path length, and tornado direction. The design basis tornado with a windspeed of 360 mph [26] was used as the maximum intensity event. Thus, as noted in Table III-3, the F'6 tornado intensities were specified to have a windspeed interval of from 277 to 366 mph and an occurrence rate of 1.765×10^{-7} per square mile per year. The angular difference of 15 degrees clockwise between plant north and true north was also accounted for in the directional tornado data input relative to the plant target model and missile zone geometry.

TABLE III-3. TORNADO INTENSITY INTERVALS AND OCCURRENCE RATES

Tornado Intensity (F'-Scale)	Windspeed Interval (mph)	Occurrence Rate (/sq. mi. yr.)
F'0	40-73	1.314×10^{-4}
F'1	73-103	1.325×10^{-4}
F'2	103-135	1.134×10^{-4}
F'3	135-168	4.720×10^{-5}
F'4	168-209	1.412×10^{-5}
F'5	209-277	2.338×10^{-6}
F'6	277-360	1.765×10^{-7}
All	40-360	4.412×10^{-4}

IV. RESULTS AND CONCLUSIONS

A. Tornado Windspeed Exceedance Probabilities

Using the method described in Section II.B, the tornado windspeed probabilities for the cable tray bridge structures have been calculated using the TORRISK code. These probabilities have been estimated by simulating tornado occurrences at the Oyster Creek Station corresponding to 1,000 tornadoes for each F-scale intensity from F1 to F6. The upperbound windspeed for F6 intensity tornadoes was assumed to be 360 mph. Table IV-1 summarizes the windspeed exceedance probabilities for these two structures at a height 62 ft above plant grade. The statistical confidence bounds represent the uncertainties in the mean probability estimation resulting from a sample size of 1,000 tornadoes in the Monte Carlo analysis. A plot of exceedance probability versus fastest quarter-mile windspeed is given in Fig. IV-1. From this plot, the windspeed corresponding to a 10^{-7} annual exceedance probability is estimated as 300 mph. It is emphasized that this windspeed function is based on conservative F-scale windspeed transformations and a 360 mph upperbound F6 windspeed. Our best-estimate of the tornado windspeeds would correspond to about a 50 mph shift to the left for the higher windspeeds, principally due to updated windspeeds [4] based on engineering damage asessments and photogrammetric analyses.

B. Tornado Missile Damage Probabilities

Missile impact and damage probabilities to the cable tray bridge structures have been estimated using the TORMIS computer code simulation methodology. The simulations were performed in two phases. The initial phase involved checking the plant, missile, and simulation parameter inputs. Over

TABLE IV-1. TORNADO WINDSPEEDS AT 62 FT ABOVE GRADE
PROBABILITIES AND STATISTICAL CONFIDENCE BOUNDS

Windspeed (mph)		Probabilities of Tornado Windspeed Exceedance (per yr)		
Fastest Mile	Fastest Qtr. Mile	Lower Bound 95% Confidence Interval	Mean	Upper Bound 95% Confidence Interval
67	73	2.97×10^{-4}	3.50×10^{-4}	4.03×10^{-4}
98	112	9.56×10^{-5}	1.03×10^{-4}	1.11×10^{-4}
136	157	3.27×10^{-5}	3.55×10^{-5}	3.83×10^{-5}
188	206	7.57×10^{-6}	8.33×10^{-6}	9.09×10^{-6}
228	260	5.77×10^{-7}	6.14×10^{-7}	6.51×10^{-7}
283	318	8.74×10^{-8}	2.97×10^{-8}	3.20×10^{-8}
303	340	1.17×10^{-8}	1.33×10^{-8}	1.48×10^{-8}

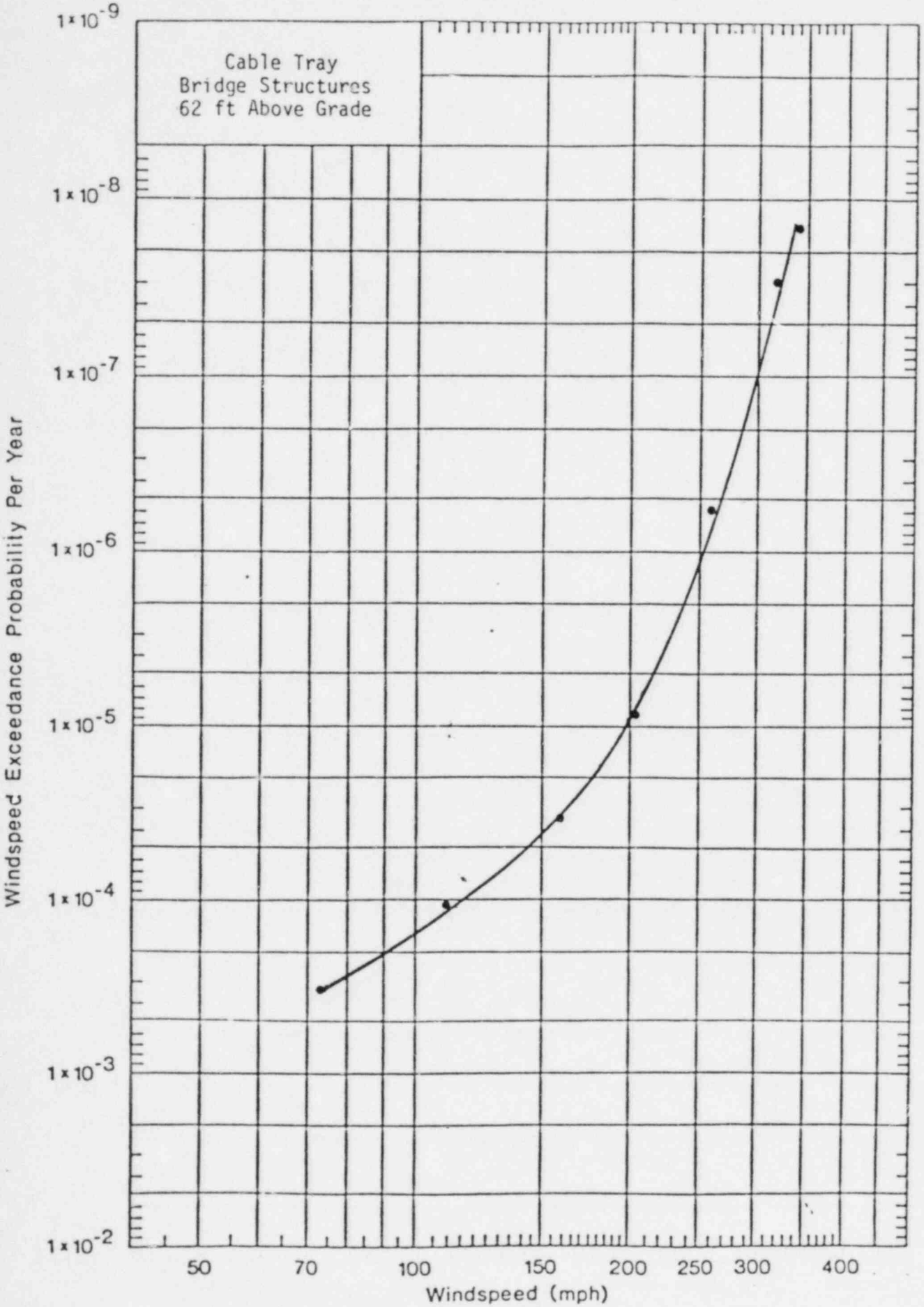

Figure IV-1. Tornado Windspeed Exceedance Probabilities

10,000 missile histories were simulated with F'6 tornadoes (318-360 mph) striking the plant. The bridge plate thicknesses were specified as 0.50, 1.00, 1.50, and 2.00 inches for this phase. Variance reduction parameters were chosen based on previous plant case studies in Ref. 8. The results were successful in that missile impacts were scored on these two rather small and elevated targets. However, no perforations of even the lowest plate thickness (0.50 in.) were obtained for the 10,000 simulations. It is likely that most of the impacts corresponded to oblique and noncollinear impact orientations with limited perforation capability. Based on these results, the design plate thicknesses were changed to 0.25, 0.50, 0.75, and 1.00 inches for the second phase simulations.

Using the reduced plate thicknesses, a total of 32,000 missiles were simulated from F'2 to F'6 tornado intensities. A stratified sampling procedure was employed in which more histories were run for the higher intensity tornadoes. The simulation consisted of 8,000 histories for F'6, 8,000 for F'5, 6,000 for F'4, 5,000 for F'3, and 5,000 for F'2 tornadoes. Tornadoes weaker than F'2 were not simulated because the low windspeeds (< 112 mph) were assumed to be negligible contributors to the bridge plate perforation probability.

The results of the TORMIS simulation are summarized in Table IV-2. The probabilities that the bridges are impacted by one or more of the postulated tornado missile are estimated as 1.75×10^{-5} and 5.16×10^{-5} per year for Bridges 1 and 2, respectively. The probability that either bridge is impacted is estimated as 6.06×10^{-5} per year and the probability that both bridges are impacted in the same tornado event is estimated as 9.94×10^{-6} per year. These impacts are largely due to potential missile sources originating from

TABLE IV-2. BRIDGE STRUCTURE IMPACT AND PLATE PERFORATION PROBABILITIES

Target	Tornado Intensity	Impact			Perforation[2], t = 0.25 in.			Perforation, t = 0.50 in.			Perforation, t = 0.75 in.		
		Lower Bound[1]	Mean	Upper Bound	Lower Bound	Mean	Upper Bound	Lower Bound	Mean	Upper Bound	Lower Bound	Mean	Upper Bound
1	F2	0	8.93×10^{-7}	2.38×10^{-6}	0	3.13×10^{-7}	8.87×10^{-7}		*[3]			*	
	F3	0	1.39×10^{-5}	3.14×10^{-3}	0	*			*			*	
	F4	0	1.85×10^{-6}	3.92×10^{-7}	0	2.20×10^{-7}	6.33×10^{-7}		*			*	
	F5	2.94×10^{-7}	8.68×10^{-7}	1.46×10^{-6}	0	3.09×10^{-10}	7.76×10^{-10}	0	2.42×10^{-10}	6.99×10^{-10}	0	1.32×10^{-10}	3.81×10
	F6	2.04×10^{-9}	2.03×10^{-8}	3.85×10^{-8}	0	5.02×10^{-9}	1.46×10^{-8}	0	3.01×10^{-9}	8.68×10^{-9}		*	
	ALL	0	1.75×10^{-5}	3.53×10^{-5}	0	5.56×10^{-7}	1.25×10^{-6}	0	3.25×10^{-9}	8.94×10^{-9}	0	1.33×10^{-10}	3.81×10
2	F2	1.80×10^{-5}	2.05×10^{-5}	3.93×10^{-5}	0	2.18×10^{-8}	5.96×10^{-8}	0	4.86×10^{-10}	1.38×10^{-9}		*	
	F3	0	3.10×10^{-5}	7.35×10^{-5}	0	7.93×10^{-8}	2.26×10^{-7}		*			*	
	F4	0	9.60×10^{-7}	2.31×10^{-6}	0	9.57×10^{-8}	2.76×10^{-7}		*			*	
	F5	1.30×10^{-7}	4.48×10^{-7}	7.62×10^{-7}	0	6.53×10^{-8}	1.51×10^{-7}	0	1.07×10^{-8}	3.09×10^{-8}		*	
	F6	0	7.03×10^{-8}	1.73×10^{-7}	8.47×10^{-10}	3.85×10^{-9}	6.84×10^{-9}	0	5.72×10^{-10}	1.44×10^{-9}	0	6.67×10^{-11}	1.93×10
	ALL	5.20×10^{-6}	5.16×10^{-5}	9.80×10^{-5}	3.00×10^{-8}	2.67×10^{-7}	5.04×10^{-7}	0	1.18×10^{-8}	3.20×10^{-8}	0	6.67×10^{-11}	1.93×10
1∪2	F2	2.90×10^{-6}	2.13×10^{-5}	3.99×10^{-5}	0	3.47×10^{-7}	8.99×10^{-7}	0	4.86×10^{-10}	1.38×10^{-9}		*	
	F3	0	3.63×10^{-5}	7.85×10^{-5}	0	7.93×10^{-8}	2.26×10^{-7}		*			*	
	F4	0	1.97×10^{-6}	4.09×10^{-6}	0	2.92×10^{-7}	8.40×10^{-7}		*			*	
	F5	3.99×10^{-7}	9.60×10^{-7}	1.52×10^{-6}	0	6.59×10^{-8}	1.51×10^{-7}	0	1.09×10^{-8}	3.12×10^{-8}	0	1.32×10^{-10}	3.81×10
	F6	0	8.11×10^{-8}	1.84×10^{-7}	0	8.87×10^{-9}	1.84×10^{-8}	0	3.58×10^{-9}	9.25×10^{-9}	0	6.67×10^{-11}	1.93×10
	ALL	1.45×10^{-5}	6.06×10^{-5}	1.07×10^{-4}	0	7.93×10^{-7}	1.59×10^{-6}	0	1.50×10^{-8}	3.59×10^{-8}	0	1.99×10^{-10}	4.79×10
1∩2	F2	0	8.32×10^{-8}	2.38×10^{-7}	0	6.79×10^{-9}	1.94×10^{-8}		*			*	
	F3	0	8.66×10^{-6}	2.43×10^{-5}		*			*			*	
	F4	0	8.36×10^{-7}	2.07×10^{-6}	0	2.40×10^{-8}	6.88×10^{-8}		*			*	
	F5	4.06×10^{-8}	3.56×10^{-7}	6.74×10^{-7}		*			*			*	
	F6	1.49×10^{-9}	9.38×10^{-9}	1.73×10^{-8}		*			*			*	
	ALL	0	9.94×10^{-6}	2.56×10^{-5}	0	3.08×10^{-8}	7.76×10^{-8}		*			*	

Lower and Upper Bounds correspond to 95 percent statistical confidence bounds.
No perforations of targets 1 or 2 were obtained for t > 0.75 in.
* denotes no perforations were obtained.

cladding and support structure failure from targets 3 and 7. No impacts by vehicle type missiles lifted up from ground elevations were recorded. The 95 percent statistical confidence bounds resulting from the Monte Carlo sample size are also shown in Table IV-2. For these simulation parameters, the upperbound is about twice the esimated mean value.

The summary in Table IV-2 indicates that plate perforations are much less likely than impacts. For example, the probability of perforating a 0.25 inch plate wall of either Bridge 1 or 2 is estimated as 7.93×10^{-7} per year. The probability of perforating 0.25 inch plate on both structures in the same tornado event is about an order of magnitude less, or about 3.08×10^{-8} per year. This reduction results from the orientation of the two structures and the fact that Bridge 2 tends to shield the south wall of Bridge 1. Hence, Bridge 1 is most vulnerable on its roof plate, whereas Bridge 2 is vulnerable on both the roof and south wall. From Table IV-2, the perforation probabilities reduce considerably with increasing plate thickness. For 0.75 inch plate, the probability that either strucutre is perforated is estimated as about 1.99×10^{-10} per year. Simultaneous damage to both bridges for plate thickness of 0.50 in or greater were not obtained in these simulations.

Plots of plate thickness versus perforation probability are given in Fig. IV-2 for the event that at least 1 of the 2 bridges are damaged ($1 \cup 2$) and the event that both bridges are damage ($1 \cap 2$) in the same tornado strike. The estimated annual probabilities and upperbound Monte Carlo uncertainties are shown. These results indicate that only minimal plate thicknesses are needed, particularly for damage to the redundant structures by missiles generated in the same tornado strike. To reflect the uncertainties in the input data, adjustments to the curves are suggested for design applications in the absence

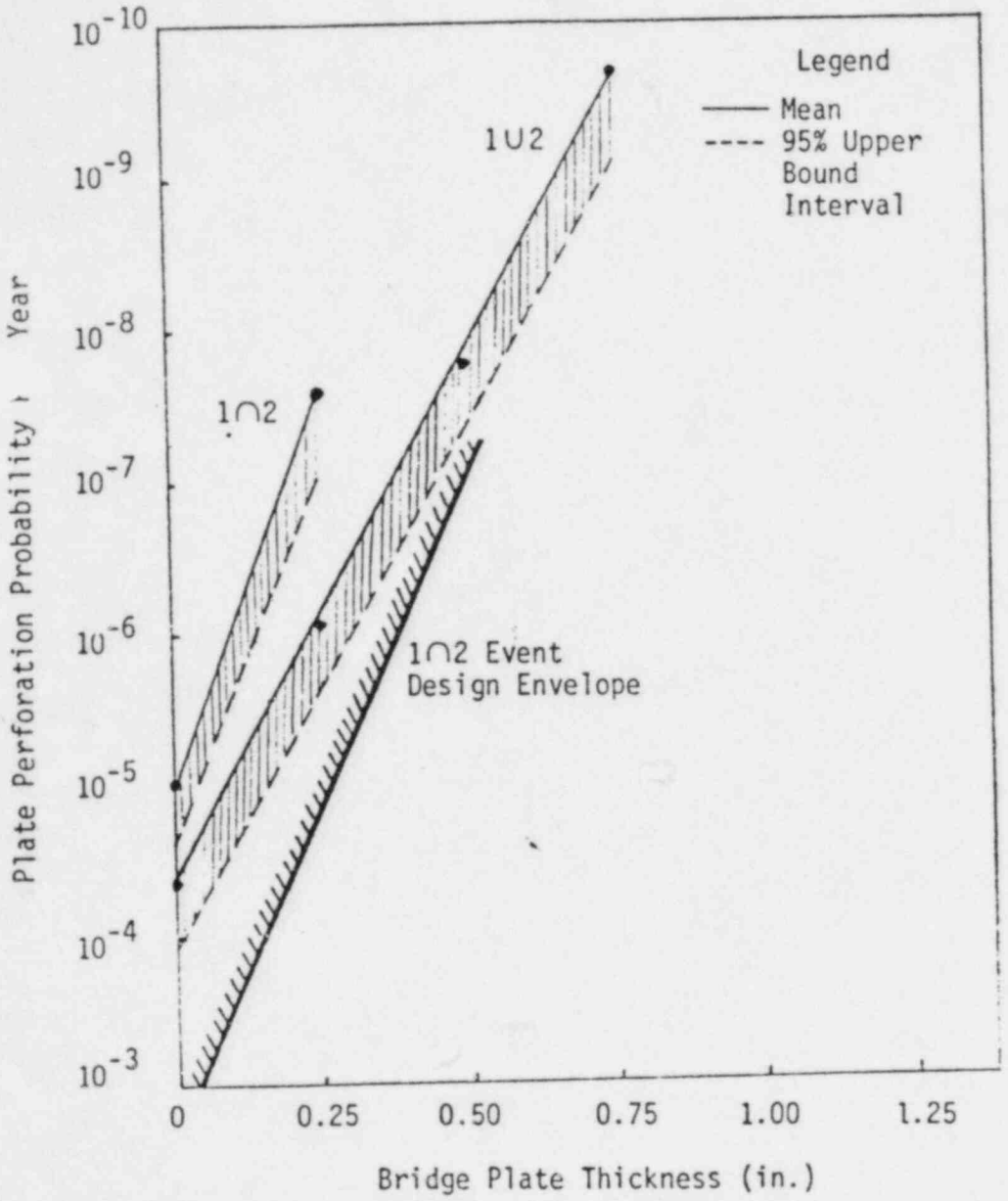

Figure IV-2. Bridge Plate Perforation Probability

of more detailed sensitivity analyses. If we assume that the slope of these curves are approximately correct, then a conservative adjustment is to force the $1 \cap 2$ perforation event through the tornado strike probability for > F1 events, which is 3.50×10^{-4} per year (from Table IV-1). Using an uncertainty interval twice that reported in Table IV-2, we obtain the design envelope for the $1 \cap 2$ event in Fig. IV-2. It is our opinion that even if additional simulations and sensitivity analyses were performed for this plant, this envelope would prove to be adequate for design purposes. Hence, a plate thickness of 0.50 inches would be expected to resist simultaneous perforation of both bridges with a 10^{-7} annual exceedance probability. It is noted that these results appear reasonable when one considers that 0.80 inches of plate thickness are sufficient to stop the NRC steel missile penetrators at NRC velocities and assuming normal, collinear, and non-spinning impacts. The vehicle missile, as noted earlier, is not a threat to these bridges, which are some 50 ft above grade and the wood plank missile can only perforate about 0.39 inches at the NRC velocity (see Appendix A). Thus, when one considers that the probability of simultaneous hits on these structures with missiles at peak velocity and oriented for maximum penetration is quite small, the 0.50 inch plate thickness is conservative for these elevated structures.

V. REFERENCES

1. Twisdale, L.A. et al., "Tornado Missile Risk Analysis," EPRI NP-768 (Vol. I) and EPRI NP-769 (Vol. II), Electric Power Research Institute, Palo Alto, California, May 1978.

2. Twisdale, L.A., W.L. Dunn, and T.L. Davis, "Tornado Missile Transport Analysis," Journal of Nuclear Engineering & Design, 51 (1979).

3. Dunn, W.L. and L.A. Twisdale, "A Synthesized Windfield Model for Tornado Missile Transport," Journal of Nuclear Engineering & Design, 52 (1979).

4. Twisdale, L.A., "Tornado Data Characterization and Windspeed Risk," Journal of the Structural Division, ASCE, Vol. 104, No. ST10, October, 1978.

5. Twisdale, L.A., "A Risk-Based Design Against Tornado Missiles," Proceedings of the Third ASCE Specialty Conference on Structural Design of Nuclear Plant Facilities, Boston, Mass., April 1979.

6. Twisdale, L.A., "Probabilistic Considerations in Missile Impact Assessment," Proceeding of the International Seminar on Probabilistic Design of Nuclear Power Plants, San Fransisco, Calif., August 1977.

7. Twisdale, L. A., "An Assessment of Tornado Windfied Characteristics For Missile Loading Prediction," Proceedings of Fourth U.S. National Conference on Wind Engineering Research, University of Washington, Seattle, Washington, July 1982.

8. Twisdale, L. A., and Dunn, W. L., "Tornado Missile Simulation NP-440, and Design Methodology," EPRI NP=2005, Electric Power Research Institute, Palo Alto, California, August 1981.

9. Twisdale, L. A., "Regional Tornado Data Base and Error Analysis," Preprint, AMS 12th Conf. on Severe Local Storms, San Antonio, Texas, January 1982.

10. Wen, Y.K., and Chu, S.L., "Tornado Risks and Design Wind Speed," Journal of the Structural Division, Proceedings ASCE, Volume 99, No. ST12, December 1973.

11. Fujita, T.T., "Proposed Characterization of Tornadoes and Hurricanes by Area and Intensity," The University of Chicago, SMRP Research Paper No. 91, February 1971.

12. Fujita, T. T., "Workbook of Tornadoes and High Winds for Engineering Applications," University of Chicago, SMRP Research Paper 165, September 1978.

13. Redmann, G. H., et al., "Wind Field and Trajectory Models for Tornado-Propelled Objects," Electric Power Research Institute, Palo Alto, California, NP-748, May 1978.

14. Fujita, T. T., "Graphic Examples of Tornadoes," Bulletin of the American Meteorological Society, Vol. 57, No. 4, April 1976.

15. Fujita, T. T., and Wakimoto, "Red River Valley Tornado Outbreak of April 10, 1979," Mapping for SESAME, University of Chicago, May 1979.

16. Fujita, T. T., "Preliminary Report of The Bossier City Tornado of December 3, 1978," SMRP Research Paper No. 169, January 1979.

17. Fujita, T. E., "Aerial Survey of Grand Gulf Plant and Vicinity After the April 17, 1978 Tornado," SMRP Research Paper No. 162, May 1978.

18. Forbes, G. S., "The Cabot, Arkansas Tornado of March 29, 1978," SMRP Research Paper No. 167, University of Chicago, August 1978.

19. Gwaltney, R. C., "Missile Generation and Protection in Light-Water-Cooled Power Reactor Plants," USAEC Reprot ORNL-NSIC-22, Oak Ridge National Laboratory, September 1968.

20. Baker, W. E., Hokanson, J. C., and Cervantes, R. A., "Model Tests of Industrial Missiles," Southwest Research Institute, San Antonion, Texas, May 1976.

21. Feller, W., An Introduction to Probability Theory and Its Applications, Volume I, 3rd Edition, John Wiley & Sons, Inc., New Your, 1968.

22. Fishman, G.S., Concepts and Methods in Discrete Event Digital Simulation, John Wiley & Sons, New York, 1973.

23. McGrath, E.J., Basin, S.L., Barton, R.W., Erving, D.C., Jaquette, S.C., and Ketler, W.R., et al., Techniques for Efficient Monte Carlo Simulation, ORNL-RSIC-38, Volumes 1, 2, 3, April 1975.

24. Nuclear Regulatory Commission, "Missiles Generated by Natural Phenomena," Section 3.5.1.4, Standard Review Plan, Revision 1, November, 1975.

25. Kelly, D. L., et al., "An Augmented Tornado Climatology," Monthly Weather Review, Vol. 106, August 1978, pp. 1172-1183.

26. Nuclear Regulatory Commission, "Design Basis Tornado for Nuclear Power Plants," Regulatory Guide 1.76, April 1974.

APPENDIX

TORMIS PERFORATION FORMULAS FOR STEEL PLATE TARGETS

APPENDIX A

TORMIS PERFORATION FORMULAS FOR STEEL PLATE TARGETS

The BRL perforation formula [19] for steel missiles impacting steel plate is used in the TORMIS simulation code and is given by [1]

$$e = \frac{W^{0.67} V^{1.33}}{10788\, d\, K_b^{1.33}} \qquad \text{(A-1)}$$

where e = plateperforation thickness, w = missile weight (lbs), V = equivalent impact velocity (ft/sec), d = effective missile diameter (in.) and K_b = steel target penetration constant, normally taken as unity.

Baker et al. conducted a series of 56 model tests of wood poles impacting sheet steel targets. Impact velocities were sought with produced threshold of perforation for each missile-target combination. The authors applied an energy method based upon the deformed structure shape and derived the following perforation equation

$$\frac{\rho_m V^2}{\sigma_y} = 1.751 \left(\frac{e}{d}\right)\left(\frac{L}{d}\right)^{-1} + 144.2 \left(\frac{e}{d}\right)^2 \left(\frac{L}{d}\right)^{-1} \qquad \text{(A-2)}$$

where ρ_m = missile density and σ_y = yield stress of steel target, L = missile length. The coefficients were derived empirically from the wood pole impact tests and a plot of the data indicates good agreement. Solving for perforation thickness in Eq. A-2 yields

$$e = .055d\left[-1.21 + \left(1.46 + 1.92 \frac{\rho_m L V^2}{\sigma_y d}\right)^{0.5}\right] \qquad \text{(A-3)}$$

which is utilized for wood missiles impacting steel targets in TORMIS. As a result of the large number of experimental tests upon which this formulation is based, Eq. A-2 is considered a better model for wood missiles than Eq. A-1, which was developed for steel missiles. It is noted that when Eq. A-2 is used for the 200 lb NRC wood plank missile impacting steel plate at 422 ft/sec, the perforation thickness is 0.35 in. as opposed to 1.44 in. using the BRL formula.